International Journal of Nanomedicine

Dovepress
Taylor & Francis Group

Open Access Full Text Article

REVIEW

Actively Targeted Nanoparticles for Enhanced Diagnosis, Treatment, and Vaccination of Tuberculosis: A Systematic Review

Johnessa Cung[1], Patihul Husni[2], Kyung Taek Oh[3,4]

[1]Undergraduate Program of Pharmacy, Faculty of Pharmacy, Universitas Padjadjaran, Jatinangor, 45363, Indonesia; [2]Department of Pharmaceutics and Pharmaceutical Technology, Faculty of Pharmacy, Universitas Padjadjaran, Jatinangor, 45363, Indonesia; [3]College of Pharmacy, Chung-Ang University, Seoul, 06974, Republic of Korea; [4]Department of Global Innovative Drugs, The Graduate School of Chung-Ang University, Seoul, 06974, Republic of Korea

Correspondence: Patihul Husni, Department of Pharmaceutics and Pharmaceutical Technology, Faculty of Pharmacy, Universitas Padjadjaran, Jatinangor, 45363, Indonesia, Email patihul.husni@unpad.ac.id

Abstract: Tuberculosis (TB) remains a leading cause of morbidity and mortality worldwide, hampered by prolonged, toxic treatment regimens that lead to poor patient adherence and drug resistance, as well as diagnostic tools that lack sensitivity and specificity. This systematic review evaluates recent advancement in actively targeted nanoparticle (NP) systems designed to improve TB diagnosis, treatment, and vaccination. Peer-reviewed studies published after 2015 focusing on NPs with active targeting capabilities were analyzed. The findings show that: ligand-functionalized NPs achieve precise, receptor-mediated targeting of infected cells, enhancing therapeutic efficacy; integrating diagnostic elements into these platforms enables rapid, sensitive biomarker detection; and antigen-loaded NPs effectively modulate immune responses, showing significant promise for novel vaccine development. Therefore, actively targeted NPs represent a transformative platform to overcome critical limitations in TB care by offering a unified strategy to improve diagnostic accuracy, therapeutic outcomes, and vaccine-induced immunity.

Keywords: carrier, ligand, surface modifier, receptor-mediated, specific

Introduction

Tuberculosis (TB) is a preventable and curable infectious disease primarily caused by bacteria of the *Mycobacterium tuberculosis* complex (MTBC),[1] which includes *M. tuberculosis, M. bovis, M. caprae, M. microti, M. africanum, M. canettii, M. orygis, M. pinnipedii, M. suricattae*, and *M. mungi*.[2] Infected individuals expel the bacteria into the air through actions such as coughing, sneezing, or spitting, as the lungs are the primary site of infection.[3] In some cases, TB can spread beyond the lungs, affecting multiple organ systems, known as extrapulmonary TB (EPTB), commonly involves the lymph nodes, pleura, genitourinary system, bones and joints, gastrointestinal tract, central nervous system, and the spine.[4] In 2023, TB was responsible for an estimated 1.25 million deaths worldwide,[1] marking a return to pre-pandemic mortality levels.

According to WHO guidelines, newly diagnosed patients continued to follow the standard 6-month regimen, which consists of isoniazid and rifampicin, with the addition of pyrazinamide and ethambutol during the initial 2-month phase (2HRZE/4HR).[5] Patients with multidrug-resistant (MDR) and extensively drug-resistant (XDR) TB can be treated with a 6-month regimen comprising bedaquiline, pretomanid, and linezolid (BPaL), offering a shorter, oral alternative to conventional MDR/XDR treatment regimens. *M. tuberculosis* (*Mtb*) exhibits a notably slow replication rate,[6] which in this case leads to the prolonged use of injections and treatment in general.[7] However, such lengthy regimens are often associated with reduced patient adherence, increasing the risk of incomplete therapy, treatment failure, and the emergence of drug-resistant strains, factors that significantly compromise the overall effectiveness of TB control efforts.[8]

Received: 17 August 2025
Accepted: 4 November 2025
Published: 2 December 2025

Graphical Abstract

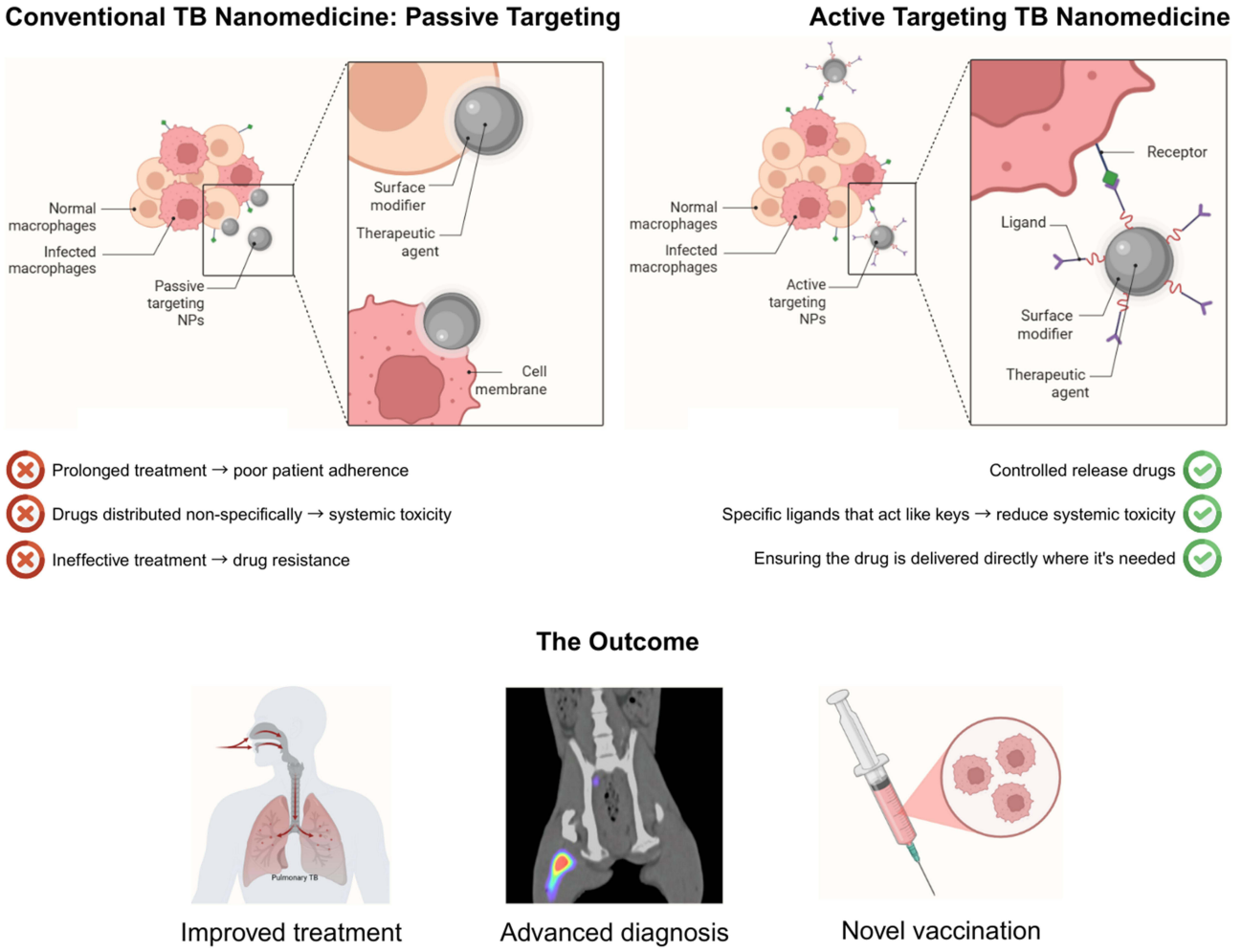

As for the TB diagnosis, sputum culture remains the gold standard due to its high sensitivity and specificity.[9] However, these traditional culture methods require prolonged incubation periods, weeks to detect *Mtb*,[10] which causes a significant delay in initiating appropriate treatment for newly diagnosed patients in order to minimize the risk of transmission to other individuals.[11,12] Recent molecular diagnostic tests, such as polymerase chain reaction (PCR), allow for the rapid and accurate identification of *Mtb* directly from sputum samples.[13] This method can be challenging in certain individuals, particularly those with a low bacterial load, common in the early stages of the disease.[14] These limitations are even more pronounced in patients suspected of having EPTB, for whom sputum-based diagnosis is often uninformative or not feasible.[15]

In response to these challenges, the growing need for novel and efficacious anti-TB diagnosis tools and treatments is essential.[6] As a drug delivery system (DDS), where therapeutic agents are encapsulated within the polymer matrix via chemical interactions,[16] NPs offer the advantages of controlled, gradual, and prolonged drug release from the biodegradable carriers,[17] and with their small size, NPs demonstrate superior cellular penetration compared to larger molecules,[18] making them promising candidates for targeted tools for TB.

Besides advances in therapy, nanotechnology has also significantly improved TB diagnostics. Due to their high surface area-to-volume ratio, nanomaterials offer abundant reactive sites, which substantially increase detection sensitivity and enable identification of *Mtb* or other MTBC even at low bacterial loads, differentiating it from the conventional

tools.[19] Nanomaterials have been utilized in various rapid diagnostic platforms, which shorten the time required for diagnosis compared to traditional methods.[20] Furthermore, nanomaterials can interact with multiple target molecules simultaneously, allowing for the detection of various TB biomarkers in a single assay.[21]

While nanomedicine offers both passive and active targeting strategies, their effectiveness in the context of TB is not equal.[22] Passive targeting, which relies on the enhanced permeability and retention effect is often hindered in TB. The complex, fibrotic structure of TB granulomas can be poorly vascularized, which limits the penetration of NPs that depend solely on leaky blood vessels to reach the site of infection.[8] In contrast, active targeting provides a specific binding that facilitates receptor-mediated endocytosis, a highly efficient uptake mechanism that can significantly increase intracellular drug concentration.[23] However, this strategy is not without its own challenges, including greater manufacturing complexity and the potential for immunogenicity.[24,25]

The potential of nanomedicine to overcome the challenges of conventional TB therapy has been the subject of several reviews, which have provided comprehensive summaries covering a wide range of nanocarriers, therapeutic strategies, and future challenges. While these works have broadly surveyed the field,[5,26,27] a dedicated and systematic analysis focused specifically on actively targeted NPs remains a key area for exploration. This review aims to fill that gap by providing a detailed evaluation of the core materials, delivery platforms, surface modifiers, and its diverse applications. By concentrating on active targeting, this work offers a focused perspective on the rational design and performance of these advanced nanomedical systems for TB.

Materials and Methods

This article review was conducted as a comparative study based on a selection of peer-reviewed research articles retrieved from online scientific databases. For this review, a systematic search was performed on PubMed, Scopus, and Google Scholar. The following keywords were used for the search: “active targeting” “nanoparticles”, “tuberculosis”, and “ligand” aiming for titles and abstracts of relevant studies.

The inclusion criteria for this review required articles to be international, original research reporting on in vitro or in vivo experimental work. Furthermore, studies needed to focus specifically on novel NP-based systems engineered for active targeting in TB and published in the English language. Conversely, studies were excluded if they were review articles, meta-analyses, book chapters, conference abstracts, or editorials. Articles published prior to 2015 were also excluded to ensure the recency of data, as were any studies not focused on the specific topic of active targeting NPs for TB. The complete article selection process is summarized in the flow diagram (Figure 1).

Core Materials of Active Targeting Nanoparticles

Active Pharmaceutical Ingredients

Several conventional TB drugs are commonly administered orally, which can lead to poor patient adherence.[18] In passive targeting formulations, active pharmaceutical ingredients (APIs) are encapsulated within biocompatible carriers.[25] These carriers improve the solubility and stability of the APIs, protect them from premature degradation, and provide sustained drug release.[28] While active targeting NPs are also encapsulated within biocompatible carriers, but coupled by ligands, which can lead to directly increased drug accumulation in infected tissues (Figure 2).[29] Building on this, researchers have found a way to make TB-based medicine more effective as a treatment as summarized in Table 1.

Rifampicin

Rifampicin (RIF) is frequently encapsulated in actively targeted NPs to overcome its significant limitations as a free drug, primarily its poor aqueous solubility and susceptibility to degradation.[63] As a first-line anti-TB agent that functions by inhibiting bacterial DNA-dependent RNA polymerase,[64] its efficacy is often hampered by its Biopharmaceutics Classification System (BCS) Class II properties. Nanoencapsulation protects RIF from first-pass hepatic metabolism and potential drug–drug interactions, ensuring more of the active drug reaches the target site.[63]

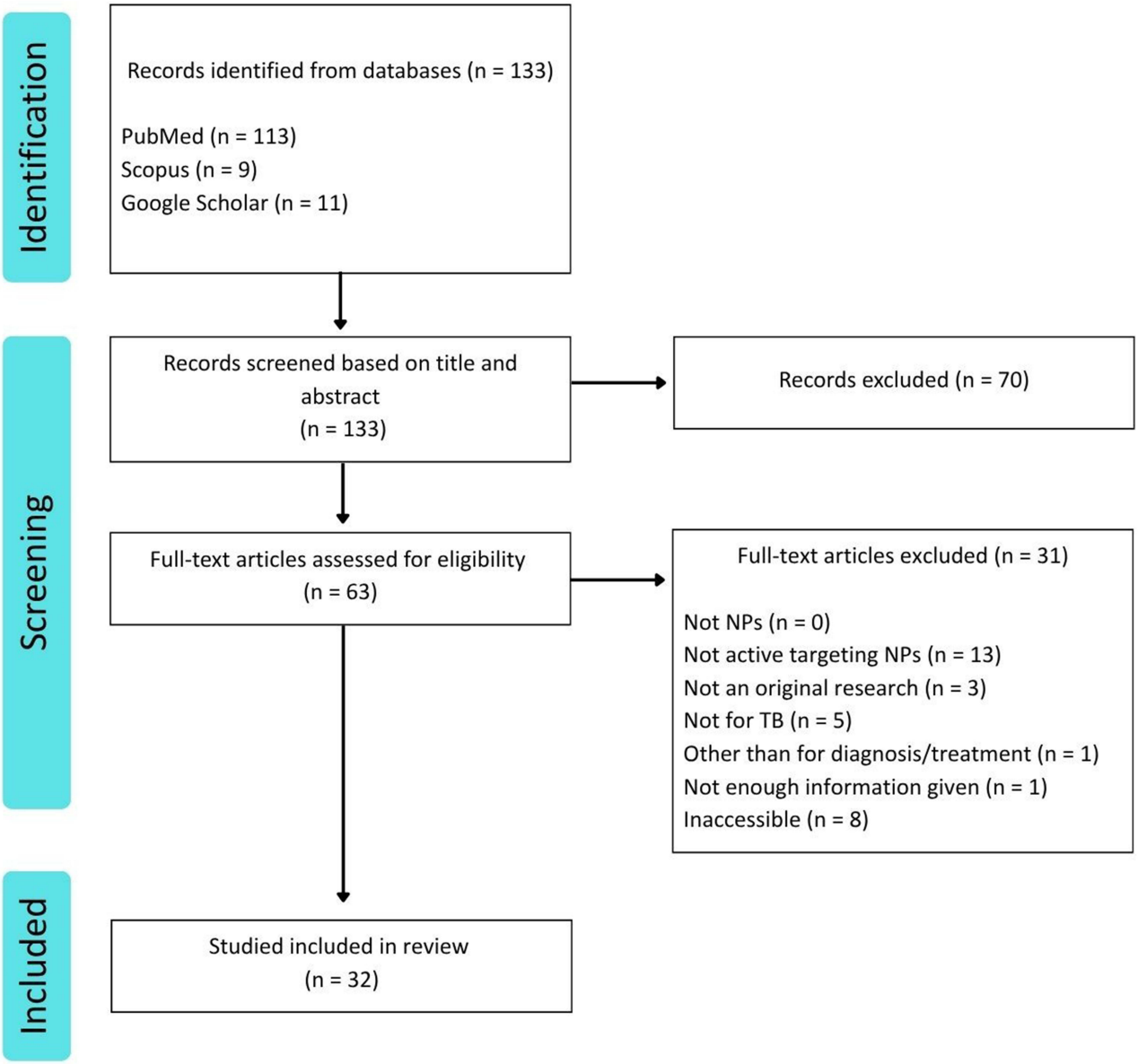

Figure 1 Flowchart of literature identification and screening process.

Isoniazid

Isoniazid (INH) is incorporated into NP systems to manage its highly variable pharmacokinetics and improve its therapeutic index.[65] As a first-line anti-TB agent, INH works by inhibiting the synthesis of mycolic acid, which is an essential component of the *Mtb* cell wall.[65,66] However, its clinical use is complicated by extensive metabolism via acetylation. Patients with "fast acetylator" status may experience a reduced therapeutic effect, while "slow acetylators" face a higher risk of hepatotoxicity.[66] Controlled release from a nanocarrier can help normalise drug exposure and mitigate these issues.

Rifampicin and Isoniazid

Co-encapsulation of RIF and INH within a single NP is a common strategy to ensure drugs reach the infection site simultaneously and to prevent chemical interactions that can reduce their stability.[67] Although INH is highly soluble, it can interact with the poorly soluble RIF under gastric conditions, leading to reduced bioavailability of both drugs when administered together in their free forms.[68]

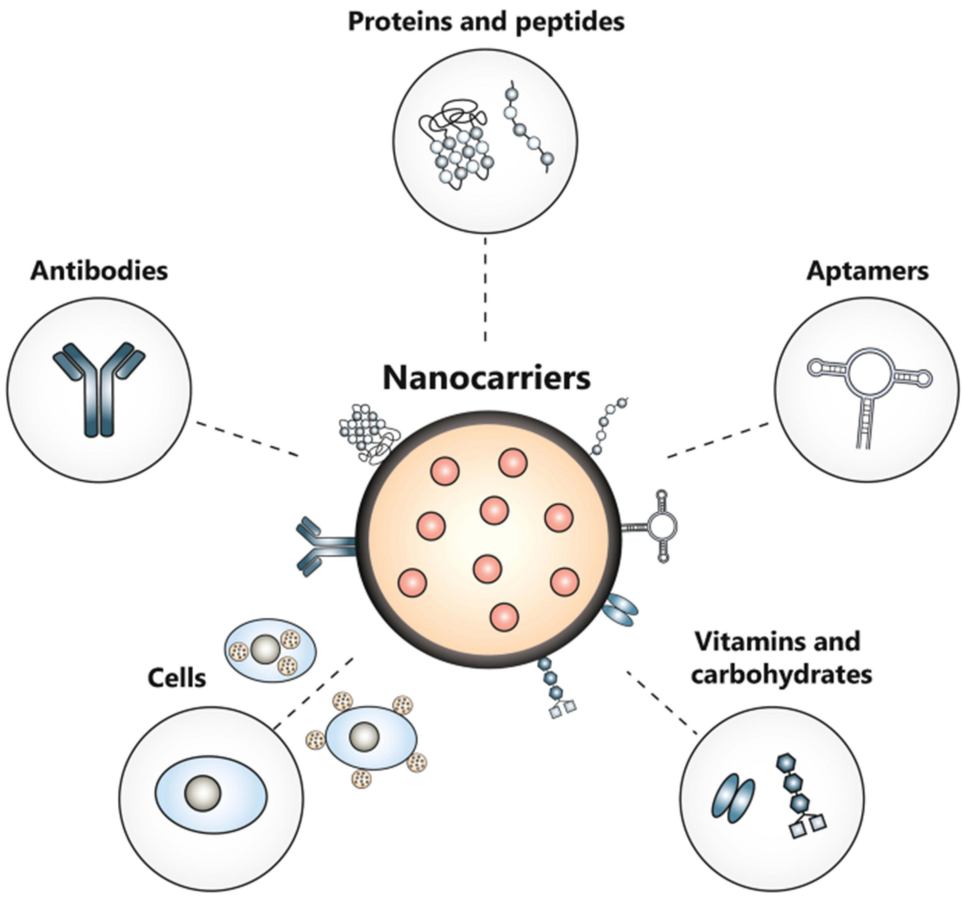

Figure 2 Active pharmaceutical ingredients encapsulated within actively targeted nanoparticles compounds.[30]

Rifapentine

Rifapentine (RPT), a long-acting rifamycin derivative, is encapsulated in NP to overcome its poor water solubility and enhance its bioavailability.[69] While RPT offers the advantage of longer half-life compared to RIF, allowing for less frequent dosing in shorter-course TB treatments, its efficacy is limited by its poor absorption following oral administration.[70]

Rifabutin

Rifabutin (RFB) is formulated into nanocarriers to address its poor aqueous solubility, which can lead to inconsistent systemic exposure.[71] This rifamycin derivative is used in TB treatment and prophylaxis against *M. avium* complex (MAC) in immunocompromised patients,[72] offering a longer half-life and greater lipophilicity than RIF.[73]

Levofloxacin

Levofloxacin (LVX) is incorporated into targeted NPs to overcome its non-specific distribution and increase drug accumulation at the site of infection.[74] As a second-line fluoroquinolone for MDR-TB, LVX distributes widely throughout the body, which often results in sub-therapeutic concentrations in infected tissues and contributes to systemic side effects.[75]

Clofazimine

Clofazimine (CFZ) is encapsulated in NPs to manage its unpredictable absorption and prevent non-specific tissue accumulation.[76] This riminophenazine antibiotic, increasingly used in MDR-TB regimens,[77] is a BCS Class II drug that tends to accumulate in fatty tissues, leading to prolonged retention and potential side effects.[76]

https://doi.org/10.2147/IJN.S557784

Table 1 Designs and Applications of Actively Targeted Nanoparticles for Tuberculosis

Active Ingredients	Core Delivery Systems	Surface Modifier	Target Receptors	Applications	Authors
None	Metallic magnetic iron oxide, gold	*M. bovis* monoclonal antibody	Cell surface and secreted antigens of *Mtb* and *M. bovis*	*Mtb* diagnostic tool	[31]
None	Gold, fullerene, polyaniline	MPT64 binding aptamers	*Mtb*-specific antigens in human serum	*Mtb* diagnostic tool	[32]
MXene	Fullerene & gold-platinum bimetallic	ESAT-6 antigen binding aptamers	*Mtb*-specific antigens in human serum	*Mtb* diagnostic tool	[33]
Tufted carbon nanotubes	Gold & fullerene	Polyaniline	IS6110 DNA sequence of *Mtb*	*Mtb* diagnostic tool	[34]
Screen printed carbon electrode	Silica	CdSe/ZnS quantum dots	*Mtb* CFP10–ESAT6 secreted protein	*Mtb* diagnostic tool	[35]
Rifampicin	Cholesteryl myristate, palmitic acid, tripalmitin	Methyl α-D-manno pyranoside	MRs on infected AMs	Inhalation TB treatment	[36]
Rifampicin	Palmitic acid	Mannose	MRs on infected AMs	Inhalation TB treatment	[37]
Isoniazid	None	Mannosylated chitosan and hyaluronic acid	CD44 receptors on infected AMs	Inhalation TB treatment	[38]
TPE-BT-BBTD	PLGA	*M. marinum* stimulated macrophages	TLRs on infected macrophages	Photothermal therapy for TB	[39]
Rifampicin	Porous polydopamine	Mannose	MRs on infected macrophages	Photothermal therapy for TB	[40]
Acr-1 antigen	Chitosan	4-SO_4-GalNAc	CLRs on macrophages surface	Vaccine against *Mtb*	[41]
None	Phosphatidylcholine & cholesterol	PEG & thioaptamers	CD44 receptors on infected macrophages	Vaccine against TB	[42]
Mtb fusion protein	PLGA-PEG	Triantennary N-Acetylgalactosamine & SR717	ASGPRs on infected DCs	Vaccine against *Mtb*	[43]
Mycolic acid	Polyethylene glycol-block-polypropylene sulfide	Acid-sensitive fluorophore	CD1b receptors on infected DCs	Vaccine against TB	[44]
Rifapentine	PLGA-PEG	TC-PEG	Bone tissue	Bone TB treatment	[45]
Isoniazid & rifampicin	PEG	Alendronate	*Mtb* infected bone marrow mesenchymal stem cells	Bone TB treatment	[46]
Rifampicin	Chitosan	Mannose	MRs on infected AMs	Bone & joint TB treatment	[47]
Rifampicin	Exosomes from bone marrow mesenchymal stem cells	ANG peptide	BBBs	CNS-TB treatment	[48]
Clofazimine	PLGA-PEG	TfRs binding peptide	TfRs receptors in BECs	CNS-TB treatment	[49]

Perchlozone©	PLGA	Single chain camel IgG	*Mtb*-infected macrophages	MDR-TB treatment	[50]
Pyridopyrimidine derivative	PLGA	Palmitoylated tuftsin	dUTPase enzyme in *Mtb*	MDR-TB treatment	[51]
Clofazimine	Chitosan	Mannose	MRs on infected AMs	MDR-TB treatment	[52]
Levofloxacin	PLGA & soya lecithin	Mannose	MRs on infected AMs	TB treatment	[53]
Rifampicin	Manganese dioxide	Tuftsin & hyaluronic acid	*Mtb*-infected macrophages	TB treatment	[54]
Rifampicin	Precirol®, miglyol-812, polysorbate 60	Mannose	MRs on infected AMs	TB treatment	[55]
Gallium (III)	PLGA	Folic acid	Specific receptors on infected MDMs	TB treatment	[56]
Rifabutin	Precirol®, miglyol-812, polysorbate 60	Mannose	MRs on infected AMs	TB treatment	[57]
Rifampicin & d-Pinitol	Chitosan	Curdlan sulphate	Dectin-1 receptor on infected macrophages	TB treatment	[58]
TB515	PLGA	Pluronic F127 & tuftsin	*Mtb*-infected macrophages	TB treatment	[59]
Rifampicin	Tocopherol succinate	Hyaluronic acid	CD44 receptors on infected AMs	TB treatment	[60]
Rifampicin	PLGA	1,3-β-glucan & rhodamine	Dectin-1 receptors on infected macrophages	TB treatment	[61]
Isoniazid	PLGA	Mycolic acids	*Mtb*-infected macrophages	TB treatment	[62]

Abbreviations: *M. bovis, Mycobacterium bovis; Mtb, Mycobacterium tuberculosis*; MPT64, *Mycobacterium tuberculosis* protein 64; ESAT-6, Early secreted antigenic target 6 kDa; IS6110, Insertion sequence 6110; CdSe/ZnS, Cadmium selenide/Zinc sulfide; CFP10, Culture filtrate protein 10 kDa; MRs, Mannose receptors; AMs, Alveolar macrophages; TB, Tuberculosis; CD44, Cluster of differentiation 44; TPE-BT-BB, Tetraphenylethylene-benzothiadiazole-bis-benzothiadiazole; PLGA, Poly(lactic-co-glycolic acid); *M. marinum, Mycobacterium marinum*; TLRs, Toll-like receptors; Acr-1, Alpha-crystallin-1 antigen; 4-SO_4-GalNAc, 4-sulfate-N-acetylgalactosamine; CLRs, C-type lectin receptors; PEG, Polyethylene glycol; ASGPRs, Asialoglycoprotein receptors; DCs, Dendritic cells; CD1b, Cluster of differentiation 1b; TC, Tetracycline; ANG, Angiotensin; BBBs, Blood brain barriers; CNS-TB, Central nervous system tuberculosis; TfRs, Transferrin receptors; BECs, Brain endothelial cells; IgG, Immunoglobulin G; MDR-TB, Multidrug resistant tuberculosis; dUTPase, Deoxyuridine triphosphatase; MDMs, Monocyte-derived macrophages; Dectin-1, Dendritic cell-associated C-type lectin-1.

Perchlozone©

The novel anti-TB agent Perchlozone© (PCZ) requires a nanocarrier system to mitigate its poor water solubility, low penetrability, and systemic toxicity at effective doses.[50] PCZ, used in drug-resistant TB regimens, functions by inhibiting mycolic acid synthesis to disrupt the bacterial cell wall.[78]

Gallium(III)

The metal-based agent Gallium(III) is formulated into NPs to address its poor solubility, instability at physiological pH, and non-specific biodistribution.[79] Gallium(III) shows promise against *Mtb* through its "Trojan horse" mechanism, where it mimics ferric iron (Fe^3+) to disrupt essential iron-dependent enzymatic pathways in bacteria.[80] Gallium competes with iron for uptake, but unlike iron, it cannot participate in redox reactions.[79]

Nanomaterials

Nanomaterials, defined as materials with at least a dimension in the range of 1–10 nm.[81] These properties include enhanced surface area-to-volume ratios, quantum effects, and tunable surface functionalities.[82] Zero-dimensional (0D) nanostructure, offering isotropic properties suitable for uniform ligand attachment. One-dimensional (1D) nanostructure, providing anisotropic properties that can influence cellular uptake and biodistribution. Two-dimensional (2D) nanostructure, characterized by their extensive planar surface, facilitating multivalent interactions with target receptors. Three-dimensional (3D) nanostructure offer high surface areas and the capacity for multi functionalization, enabling complex targeting strategies (Figure 3).[83]

MXenes

MXenes are utilized in diagnostic sensors for their 2D graphene-like structure and rich surface chemistry, which are ideal for ligand conjugation.[85] Derived from layered transition metal carbides or nitrides, these sheets possess hydrophilic surfaces and excellent electrical conductivity,[86] making them highly effective for biosensing applications.[85]

Carbon Nanotube

Carbon nanotubes (CNTs) are employed in targeted systems for both drug delivery and photothermal therapy (PTT) due to their unique structural and optical properties.[87] Their hollow tubular shape allows for the loading therapeutic agents, while their large surface area is well suited for surface modification.[88] Furthermore, CNTs strongly absorb near-infrared (NIR) light, enabling their use in deep-tissue imaging and PTT applications.[89]

Screen-Printed Carbon Electrode

Screen-printed carbon electrodes (SPCEs) serve as compact, low-cost, and disposable platforms for the development of advanced electrochemical biosensors for TB.[90] These 2D platforms integrate working, reference, and counter electrodes onto a single substrate,[91] offering chemical stability and scalability for detecting TB biomarkers at ultralow concentrations.[92]

Derivatives

Derivatives, are chemically modified compounds derived from a parent structure to alter or enhance specific properties. Their primary function is to tailor the physicochemical characteristics of NPs, such as solubility, size, surface charge, and stability for target applications.[93] Derivatives can facilitate ligand–receptor interactions that promote selective uptake by infected tissues.[94] In contrast, derivatives in free form often suffer from poor solubility, rapid clearance, and lack of specificity, limiting their therapeutic utility. Incorporating these derivatives into NP systems overcomes these limitations by protecting them from degradation and enabling controlled, site-specific release.[95]

TPE-BT-BBTD

TPE-BT-BBTD is used as the core of biomimetic NPs designed for deep-tissue imaging and targeted therapy. This molecule possesses aggregation-induced emission (AIE) properties, leading to strong absorption in the NIR-II region ideal for imaging with low background interference.[96] In a novel approach, these NPs were coated with membranes derived from *Mtb*-stimulated macrophages to achieve highly specific targeting.[96] A recent study demonstrated that pre-stimulating macrophages with a viral pathogen led to the upregulation of key pathogen-recognition receptors on the cell surface.[96] NPs coated with these activated

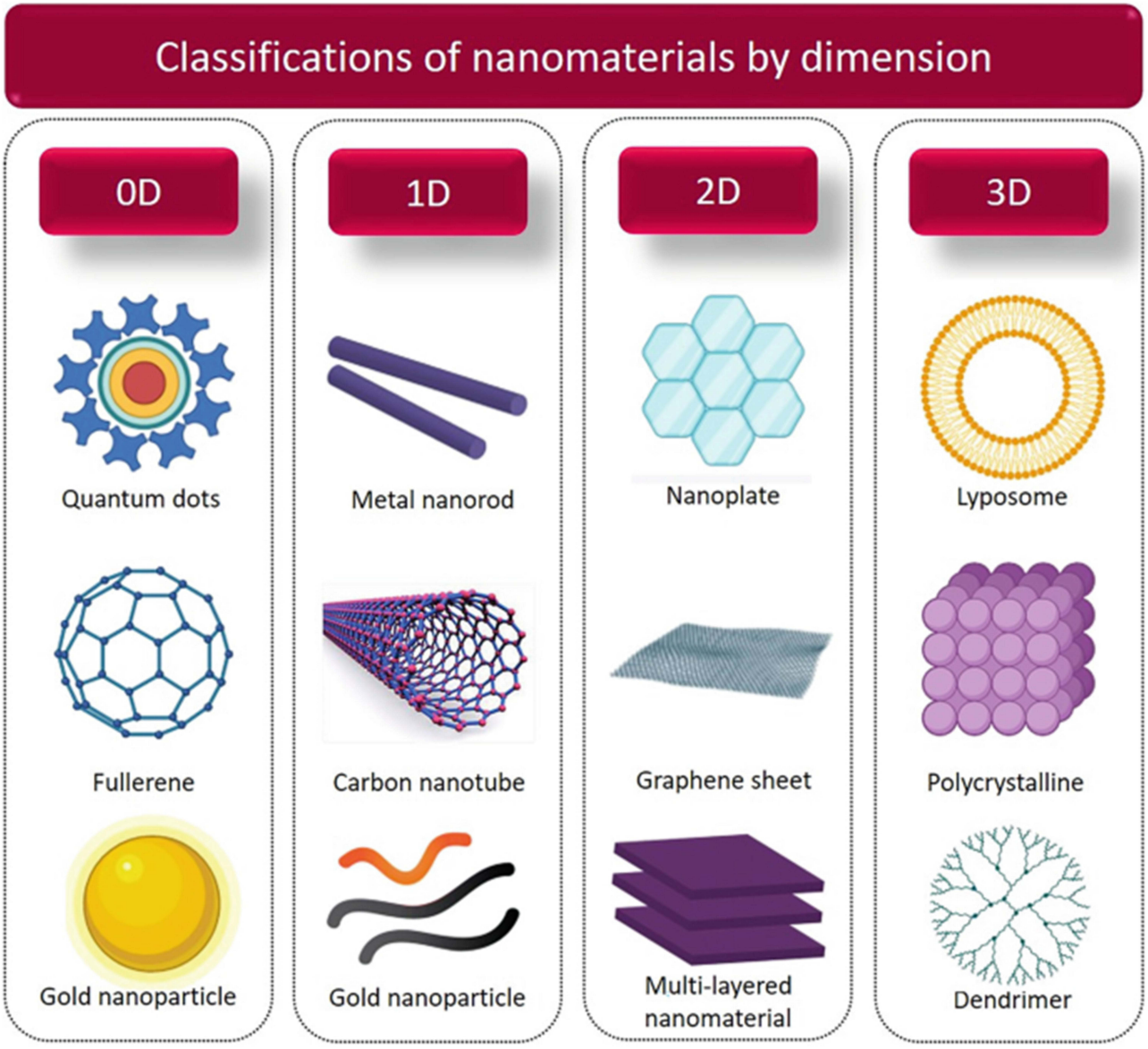

Figure 3 Classification of nanomaterials based on their dimensionality.[84]

membranes showed vastly superior targeting and retention at infected lesions, leading to more effective light-driven theragnostics.[97]

TB515

The drug candidate TB515, a coumaron derivative[98] targeting the *Mtb* dUTPase enzyme,[99] is encapsulated in NPs to overcome its poor aqueous solubility and limited cellular uptake.[100] Its intrinsic fluorescence also allows for the tracking of cellular uptake without the need for additional fluorescent labels.[101]

Pyridopyrimidine

Pyridopyrimidine and its derivative, TB820,[59] is incorporated into NPs to improve its pharmacokinetics and therapeutic efficacy. This class of fused heterocyclic compounds is recognized for its diverse biological activities and structural versatility in drug development.[102]

https://doi.org/10.2147/IJN.S557784

d-Pinitol

d-Pinitol, a cyclitol derived from various plant sources such as legumes and soy,[103] is formulated in a polyelectrolyte complex with RIF to create a more efficient therapy against *Mtb* strains through its immunomodulatory effects.[58] This d-Pinitol is known for its diverse pharmacological properties and ability to modulate intracellular signaling pathways.[104]

Antigens

Antigens have emerged as effective core materials or payloads in NP-based delivery systems aimed at enhancing cellular immunity, which is essential for combating intracellular pathogens such as *Mtb*. Conventional subunit vaccines often fall short in this regard, as they primarily trigger humoral responses. To overcome this, researchers have incorporated antigens into delivery vehicles to improve antigen uptake by antigen-presenting cells (APCs), facilitating efficient MHC-mediated presentation and providing stronger T-cell responses.[105] These strategies underline the importance of antigen-based nanocarriers in developing more potent and specific vaccines for TB.

Acr-1

Acr-1 antigen is used as a core material in NP vaccines to target latent TB infection.[106] Also known as α-crystallin, this antigen is critical for the long-term survival of *Mtb* under dormancy and stress,[106] making it an important immune stimulus for vaccines aimed at preventing reactivation.[41]

Mtb Fusion Proteins

Mtb fusion proteins, which combine multiple antigenic components from the pathogen,[107] are encapsulated in NPs to activate diverse T-cell populations and elicit a more comprehensive immune defense. This approach enhances specific recognition by immune cells and stimulates robust cell-mediated immunity,[108] as demonstrated, by the SR717 fusion protein in Tri-GalNAc-modified PLGA-PEG NPs, which enhanced dendritic cell activation.[43]

Mycolic Acids

Mycolic acids (MA) are incorporated into NP platforms to generate a potent Th1-type cellular immunity by targeting a unique T-cell population.[109] As the dominant lipid component of the *Mtb* cell wall, MA are recognized by CD1b-restricted T-cells,[110] and delivering them directly to APCs via nanocarriers ensures efficient intracellular processing and presentation.[111]

Nano-Core Delivery Systems of Active Targeting Nanoparticles

Nano-core delivery systems, also known as nanocarriers, can deliver drugs specifically to the site of infection or disease, thereby significantly enhancing therapeutic efficacy while minimizing systemic side effects.[112] In addition to improving solubility and bioavailability, these platforms reduce the required drug dosage, and shorten the duration of treatment.[113] The optimal parameters for synthetic polymer NPs typically include encapsulation efficiency (%EE) above 70%, drug loading (%DL) above 5%, polydispersity index (PDI) below 0.3, and zeta potentials above 30 mV (ie, either <-30 mV or >+30 mV) for good colloidal stability and heterogeneous dispersion.[114] An innovative application involves the use of nanocarriers, such as polymer, lipid, or metal-based systems (Figure 4).[25] Mentioned studies are summarized in Table 2.

Synthetic Polymer

Synthetic polymer-based NPs are formed from biocompatible and biodegradable synthetic polymers.[116] Their synthetic nature allows for reproducible large-scale production and structural customization, essential for overcoming the limitations of conventional TB therapies. Synthetic polymer-based NPs work by encapsulating anti-TB drugs, thereby increasing drug solubility, protecting against premature degradation, and improving bioavailability.[117] Furthermore, synthetic polymeric nanoparticles (PNPs) can be engineered for co-delivery of multiple drugs,[117] which is critical in TB therapy to prevent resistance.

PLGA

PLGA (poly(lactic-co-glycolic) acid) is a highly versatile polymer used in several of the reviewed systems, Li et al[39] developed BBTD@PM NPs using PLGA as a matrix to deliver a photothermal compound, with particle size of 88.1 nm

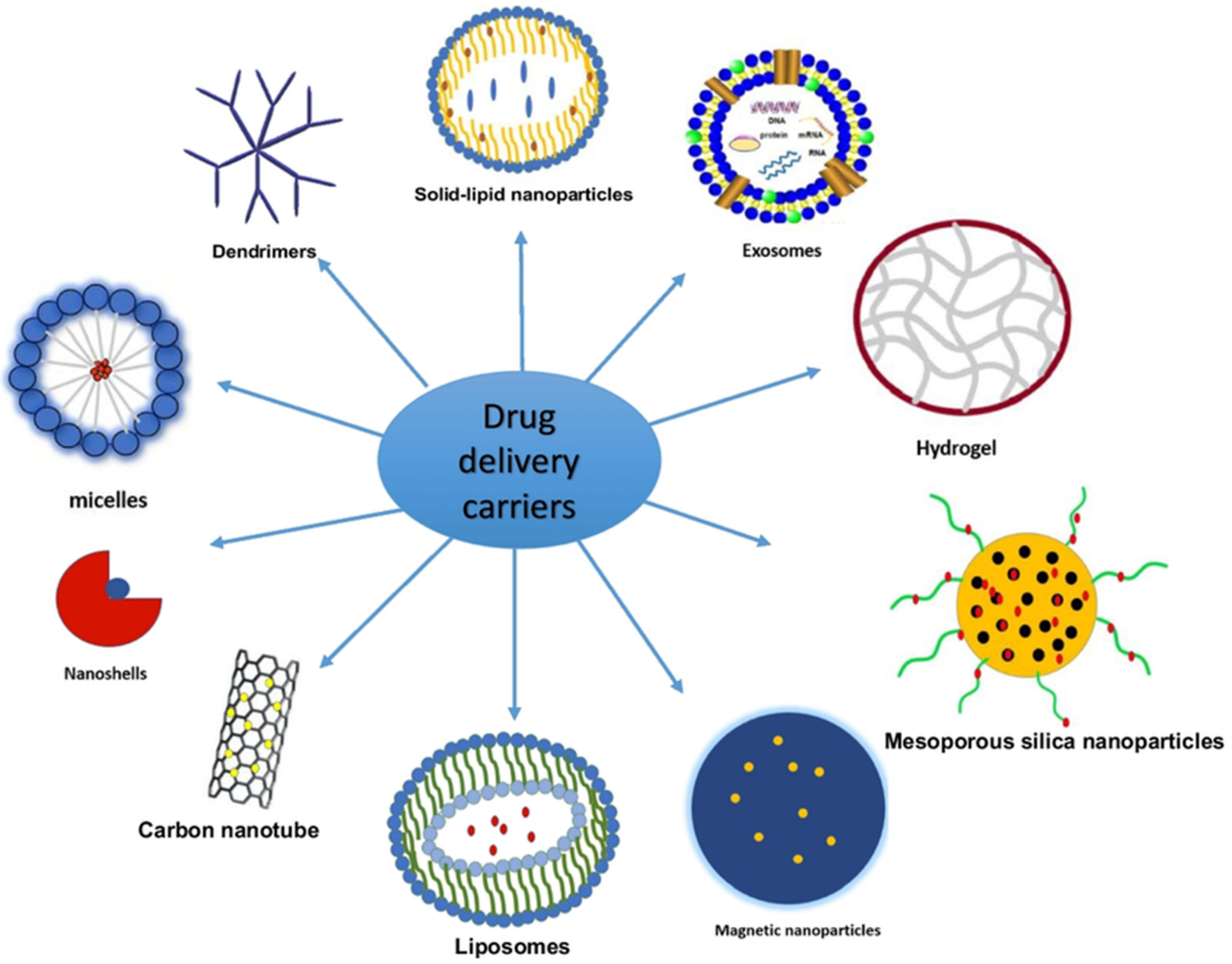

Figure 4 Types of nanocarriers used for targeted delivery.[115]

and a zeta potential of −21.3 mV, demonstrating colloidal stability for up to 15 days at 25°C. These physicochemical parameters suggest sufficient repulsion to prevent aggregation and facilitate systemic circulation. Churilov et al[50] used PLGA-related polymer (PLA) to encapsulate PCZ, achieving particle size of 170 nm, a low EE of 32%, a low DL of

Table 2 Characterization of Actively Targeted Nanoparticles for Tuberculosis

NPs Name	Particle Size (nm)	Polydispersity Index	Zeta Potential (mV)	Coupling Efficiency	Stability Evaluation	Authors
BBTD@PM	88.1	NA	−21.3	NA	15 days at 25°C	[39]
RIF-SLNas	800 ± 0.15	0.72 ± 0.12	−63.70 ± 0.23	NA	6 months at 25°C	[36]
Au–Fe_3O_4 NP-antibody bioconjugates	300.6	NA	NA	NA	NA	[31]
Rif@Man-mPDA	280	NA	−36.6	NA	NA	[40]
CNP-L	29	226	± 30.2	NA	1 month at 4°C	[41]
RPT/TC–PLGA–PEG	48.8 ± 5.8	0.21 ± 0.04	−16.8 ± 1.9	NA	3 months at 25°C	[45]

(*Continued*)

https://doi.org/10.2147/IJN.S557784

Table 2 (Continued).

NPs Name	Particle Size (nm)	Polydispersity Index	Zeta Potential (mV)	Coupling Efficiency	Stability Evaluation	Authors
LVF-CHF	471.5	NA	1.21	NA	6 months at 5 ± 3°C	[53]
CD44TA-LIP	204.9 ± 6.3	NA	−22.8 ± 1.9	NA	NA	[42]
ANG-Exo-RIF	165.9 ± 3.5	NA	−18.21 ± 2.99	15.8 ± 2.4%	NA	[48]
Tuf-Rif@HA-MnO_2	~200	NA	~30	NA	NA	[54]
PCZ-PLA	170	NA	−31	2.0 mg/g	10 days	[50]
M-NLCs-RIF	302 ± 23	0.16 ± 0.03	+36 ± 7	NA	NA	[55]
TP/GPS	238.53 ± 12.5	0.148 ± 0.03	−25.20 ± 0.29	NA	NA	[43]
NP-CFZ 5% Mal20%: Pep	149.60 ± 47.45	0.157 ± 0.040	− 10.78 ± 2.723	7.9%	NA	[49]
MXene/C60NPs/Au@Pt	NA	NA	4.46	NA	20 days at 4°C	[33]
GaF	329	0.4	+30.6	NA	NA	[56]
M-NLC-RFB	213 ± 2	0.12 ± 0.02	+37.6 ± 1.0	NA	6 months	[57]
Cfz-CS-MNS-NP	184.7 ± 2.37	0.33 ± 0.017	9.12 ± 0.08	NA	NA	[52]
SLNas/MS	740 ± 85	0.60 ± 0.05	−35.2 ± 0.1	NA	NA	[37]
CSC: D-PIN + RIF	497.32 ± 18.96	~0.1	34.5 ± 1.79	NA	NA	[58]
INH BTL	100 ± 16.3	NA	~5	NA	NA	[46]
RIF BTL	84 ± 18.4	NA	−10 to −15	NA	NA	
INH-MC/HA	303 ± 16	0.179 ± 0.04	34.3 ± 6.03	NA	1 months	[38]
MA-loaded Micelle PEG-PPS-ASF	68.13	0.140	−16.5	NA	NA	[44]
TB515-PLGA-T10Tp	200	0.15	NA	90.5%	NA	[59]
RIF-HA-TS_7	299.6 ± 12.1	0.302 ± 0.05	−30.9 ± 1.22	NA	2 weeks at 37°C	[60]
Rifampicin MCNPs	142	0.154	38.5	NA	NA	[47]
Glu-PLGA-Rh (RIF)	283.1 ± 7	0.19 ± 0.03	−28.6 ± 2	NA	NA	[61]
PLGA/INH/MA	253 ± 57	0.2 ± 0.1	−21.4 ± 4.9	NA	NA	[62]

Abbreviations: NPs, Nanoparticles; nm, Nanometers; mV, Millivolts; NA, Not available.

2 mg/g, and sufficient a zeta potential of −31 mV indicating sufficient electrostatic repulsion to maintain dispersion. Horváti et al[51] developed PLGA-pT820 with a high EE of 83% and a DL of 20.2%, making it well suited for high-dose therapeutic applications over prolonged periods, essential for MDR-TB therapy. Horváti et al[59] developed TB515-PLGA-T10Tp which had a size of 200 nm, a PDI of 0.15, and a remarkably high EE of 90.5% with that, the formulation significantly reduced intracellular *Mtb* viability, indicating strong potential for latent TB treatment. Choi et al[56] developed Gallium-loaded PLGA NPs (GaF) which had a particles size of 329 nm, a PDI of 0.4, and a zeta potential of +30.6 mV, indicating strong cationic surface charge good for interaction with negatively charged bacterial membranes. Tukulula et al[61] developed Glu-PLGA-Rh (RIF) which had a particle size of 283.1 nm, PDI of 0.19, a zeta potential of −28.6 mV, and drug release of ~10% within 24 hours, indicating a slow-release kinetic for sustained delivery. This system exemplifies the utility of PLGA in targeting C-type lectin receptors on *Mtb*-infected macrophages, offering precision

therapy within granulomatous lesions. Lemmer et al[62] developed PLGA/INH/MA which had a DL of 5% and a zeta potential of −21.4 mV, which this moderate negative charge supports phagocytic uptake.

PLGA-PEG

PLGA-PEG copolymers are used to improve both pharmacokinetics and targeting capabilities by adding a hydrophilic "stealth" layer. Liang et al[45] developed RPT/TC–PLGA–PEG NPs achieved a particle size of 48.8 ± 5.8 nm with a low PDI of 0.21, reflecting uniform distribution, an EE of 83.3%, a DL of 8.1%, and released 90% of the drug within 6 hours, suitable for immediate therapeutic application. De Castro et al[49] developed NP-CFZ 5% Mal20%: Pep, a PLGA-PEG system, which had a narrow PDI of 0.157, moderate zeta potential of −10.78 mV, and DL of 3.33%, with approximately 63.4% EE, which may be insufficient for some applications. Gong et al[43] developed a PLGA-PEG system, TP/GPS, which had an approximate size of 239 nm, PDI of 0.148, and a zeta potential of −25.2 mV, supporting stable dispersibility and immune cell interaction.

PEG

PEG-only formulations are also utilized though they may have different stability profiles. Garhyan et al[46] developed INH and RIF BTL systems that showed moderate EE of ~70% with drug releases of 70–80% over 70 hours, but their low zeta potentials suggest moderate stability and potentially short circulation times. Meanwhile, Shang et al[44] developed MA-loaded Micelle PEG-PPS-ASF which had a size of 68.13 nm, a PDI of 0.140, and a zeta potential of −16.5 mV, with a high DL of 92 ± 3% which has effectively induced DN1 and memory T-cell responses.

PLGA and Soya Lecithin

To improve the encapsulation of hydrophobic drugs, Maurya et al[53] developed LVF-CHF using PLGA and soya lecithin, which had an EE of 64.36%, DL of 15.46 ± 0.33%, and sustained drug release of ~80% over 72 hours. The combination of natural phospholipids with PLGA likely contributed to improved encapsulation of hydrophobic drugs and controlled release.

Tocopherol Succinate

As another strategy to enhance biocompatibility and targeting, Gao et al[60] incorporated tocopherol succinate into their RIF-HA-TS_7 which had a high DL of 70.01 ± 0.85%, particle size of 299.6 ± 12.1 nm, moderate PDI of 0.302 ± 0.05, and a zeta potential of −30.9 ± 1.22 mV. Drug release was nearly 79.82% within 13 hours, while maintaining high cell viability, making it suitable for targeted therapy via CD44 receptor. Finally, Fan et al[40] developed Rif@Man-mPDA with particle size of 280 nm and a zeta potential of −36.6 mV suggests high dispersibility and targeting efficacy via mannose receptors.

Natural Polymer

Natural polymer-based NPs are derived from biologically sourced macromolecules.[118] These materials are inherently biodegradable, biocompatible, and often non-immunogenic, making them attractive for drug delivery applications.[25] Natural PNPs can encapsulate both hydrophilic and hydrophobic drugs and can be chemically modified or functionalized to improve stability and allow ligand conjugation for active targeting.[52]

Chitosan

Mubin et al[41] developed CNP-L which had a very small size of 29 nm and a very high PDI of 226 ± 30.2 nm with a pretty high DL of 79%, maintaining stability for one month at 4°C suitable as a vaccine. This NPs system might be weaker on the size distribution because of its synthesis method. Prabhu et al[47] developed MCNPs loaded with chitosan had a particle size of 142 nm, a narrow PDI of 0.154, and a high zeta potential of 38.5 mV, with an EE of 70.86% and DL of 70.3% over 40 hours, this system demonstrated promising delivery efficiency. Similarly, Pawde et al[52] created Cfz-CS-MNS-NP loaded with chitosan had a size of 184.7 ± 2.37 nm in size, with a PDI of 0.33 ± 0.017, and a low zeta potential of 9.12 ± 0.08 mV, while achieving a high EE of 73.45% and sustained drug release of 70.98% over 72 hours, suggest strong therapeutic potential. Pinheiro et al[57] developed a very stable and effective M-NLC-RFB loaded with chitosan, which had a particle size of 213 ± 2 nm, with a low PDI of 0.12 ± 0.02, and high zeta potential of +37.6 ± 1.0 mV, achieved 90% EE and complete drug release within 25 hours with stability over 6 months at 25°C. Ravindran et al[58] developed RIF and d-Pinitol into chitosan (CSC: D-PIN + RIF) with a particle size of 497.32 ± 18.96 nm, a zeta potential

of 34.5 ± 1.79 mV, and a DL of 245 μg/mg, the system achieved 65% drug release in 48 hours. Although good enough for NPs, this system still needs to be improved due to its bigger particle size.

Bone Marrow-Derived Exosomes

Li et al[48] developed bone marrow-derived exosomes loaded with RIF (ANG-Exo-RIF) which were 165.9 ± 3.5 nm in size with a zeta potential of −18.21 ± 2.99 mV, the moderate negative zeta potential indicates a relatively stable colloidal suspension, but lacks information on other standard NP parameters.

Lipid Based

Lipid-based NPs composed primarily of biocompatible lipids, making them highly suitable for infectious disease.[119] Nanostructured lipid carriers (NLCs), which are made from a mix of solid and liquid lipids, offer a disordered internal structure that enhances drug loading and prevents premature drug leakage.[120] Liposomes, spherical vesicles with phospholipid bilayers, can encapsulate both hydrophilic and hydrophobic drugs and are known for their compatibility with biological membranes.[121] Nanoemulsions (NEs) are fine dispersions of oil and water stabilized by surfactants, providing high surface area, excellent drug solubility, and improved absorption, which is useful for poorly soluble TB drugs.[25] Polymeric micelles, formed from amphiphilic block copolymers, have a hydrophobic core for drug encapsulation and a hydrophilic shell that prolongs circulation time and enhances systemic stability.[122]

Liposome

Singh et al[42] developed a liposomal system, yielding NPs with a size of approximately 204.9 ± 6.3 nm and a zeta potential of −22.8 ± 1.9 mV. These parameters indicate good colloidal stability and potential for enhanced interaction with negatively charged cell membranes, the formulation's size and charge suggest suitability for cellular uptake and potential systemic circulation stability.

Nanostructured Lipid Carriers

Maretti et al[36,37] explored NLCs based on fatty acid and lipid esters. Maretti et al[36] developed solid lipid NPs assemblies (RIF-SLNas) with a size of 800 ± 0.15 nm, a PDI of 0.72 ± 0.12, and a strong negative zeta potential of −63.70 ± 0.23 mV with EE of 43.6 ± 1.86% and a DL of 14.53 ± 0.62%, the formulation remained stable for six months at 25°C and was effective in sustaining drug release. Similarly, Maretti et al[37] developed SLNas/MS with a reduced size of 740 ± 85 nm, a PDI of 0.60 ± 0.05, and a zeta potential of −35.2 ± 0.1 mV with a slightly lower EE of 36.8 ± 0.9% and DL of 9.2 ± 0.2%, these characteristics needs to be improved due to higher particle size and low %EE.

Solid-Lipid Based

Solid lipid NPs (SLNs) are composed primarily of solid lipids, or a mix of solid lipids and surfactants.[116] Unlike polymeric NPs, SLNs also offer a superior safety profile, making them especially attractive for repeated or long-term administration in chronic diseases.[123] Their structural composition enables incorporation of hydrophobic drugs into a solid lipid matrix, protecting the drug from degradation and extending its circulation half-life.[124]

Vieira et al[55] developed SLN composition of Precirol® ATO 5, Miglyol-812, and polysorbate 60 (RIF M-NLCs-RIF) which exhibited a particle size of 302 ± 23 nm, PDI of 0.16 ± 0.03, and a positive zeta potential of +36 ± 7 mV, enhancing cellular uptake. It has EE of 95 ± 2% and DL of 1.3 ± 0.1% with drug release profile of approximately 20% over 3 hours which highlights the system's biocompatibility and potential to improve drug retention at the infection site.

Metal Based or Dendrimers

Metallic-based NPs (MNPs) exhibit properties such as ultra-small size, high surface area, and inherent antibacterial activity. Their metallic cores, composed of elements like gold, silver, iron, copper, or zinc, can interact with bacterial membranes and intracellular structures, disrupting bacterial function while simultaneously delivering therapeutic agents.[25] Some metallic NPs have also shown potential for multifunctional use, enabling not only drug delivery but also gene silencing and diagnostic imaging.[125] The integration of MNPs into TB therapy offers a dual-action platform, physical disruption of bacterial integrity and controlled release of anti-TB drugs, thereby increasing therapeutic efficacy and reducing the likelihood of resistance.[126]

Gilbride et al[31] developed a hybrid platform of Au–Fe_3O_4. These NPs, sized around 300.6 nm, exploited the magnetic core for imaging and directional targeting, while the gold shell facilitated bio-recognition and enhanced stability, which is essential for TB diagnosis. Similarly, Bai et al[32] integrated gold, fullerene, and polyaniline into an electrochemical biosensor that detected TB-specific markers with high sensitivity. The synergistic conductivity of polyaniline and gold, combined with the high surface area of fullerene, allowed for amplified signals and reliable detection. Chen et al[34] developed gold–fullerene-based, their conductive metals and carbon-rich structures in signal enhancement, forming a sensitive and reproducible diagnostic method that aligns well with real-time disease monitoring. On a more therapeutic front, Huang et al[33] proposed a unique gold-platinum-fullerene nanocomposite embedded in carbon nanotube networks, engineered for both catalytic sensing and stability, with a measured zeta potential of 4.46 mV and 20-day stability at 4°C, which utilized the catalytic prowess of Pt and conductive gold-fullerene synergy to amplify biosensing performance but with low colloidal stability. Liao et al[54] developed tuftsin as the matrix for Tuf-Rif@HA–MnO_2 which had a particle size of ~200 nm and a zeta potential of approximately +30 mV. MnO_2 contributed redox-sensitive properties and potential imaging functions, while the HA coating promoted active targeting of infected cells. This design exemplifies how metallic carriers can offer both bioactivity and responsiveness within biological environments. Lastly, Bakhori et al[35] developed a silica-coated metallic NPs which had a zeta potential of –18.21 mV, suggesting a low colloidal stability, but the silica shell offered stability and biocompatibility, enhancing the overall functionality of the metallic core.

Discussion

Overall, the studies consistently demonstrate that the choice of nanocarrier fundamentally dictates the physicochemical properties and, ultimately, the therapeutic potential of the NPs systems. Synthetic polymers, particularly PLGA and its PEGylated derivatives, emerge as the most versatile platforms, frequently meeting or exceeding ideal benchmarks such as an %EE above 70% and PDI below 0.3. In contrast, while natural polymers like chitosan offer excellent biocompatibility, they often present challenges with batch-to-batch consistency looking at their PDI. Lipid-based systems, especially NLCs, offer a compelling safety profile and high storage stability, making them ideal for inhalation therapies, though they typically result in larger particle sizes compared to polymeric systems.

A significant source of heterogeneity across these studies is the inconsistent reporting of key parameters with many studies failed to report both %EE and %DL, making direct comparison of efficacy challenging. Future research should prioritize standardized characterization to allow for more robust cross-study analysis.

Surface Modifiers of Active Targeting Nanoparticles

Surface modifiers of active targeting NPs are critical elements in nanomedicine, enabling selective interaction between the NP system and specific biological targets.[127] By decorating the surface of NPs with ligands, they can recognize and bind to overexpressed receptors or cellular markers, which then can actively direct therapeutic or diagnostic agents to diseased tissues, such as infected macrophages (Figure 5).[121] This ligand–receptor interaction facilitates receptor-mediated endocytosis, leading to higher therapeutic outcomes whilst reducing their toxicity.[128] Surface modifiers can range from biological macromolecules like antibodies and peptides, to small molecules like vitamins and sugars.[129] Modifiers like PEG serve dual roles, prolonging systemic circulation by reducing opsonization while also being functionalized with targeting ligands such as folic acid or peptides.[130] Quantum dots and functional dyes, though primarily used for imaging, can also act as theragnostic agents when combined with targeting ligands.[131] Combination strategies, wherein multiple modifiers are used simultaneously, allow for synergistic effects in targeting and retention.[132] Mentioned studies are summarized in Table 2.

Protein

Protein-based surface modifiers, such as monoclonal antibodies, antibody fragments, and receptor-specific ligands, are highly valued for their specificity and strong binding affinity.[127] These large biomolecules can recognize overexpressed antigens or receptors on target cells, enabling precise delivery of therapeutic agents. Their ability to trigger receptor-

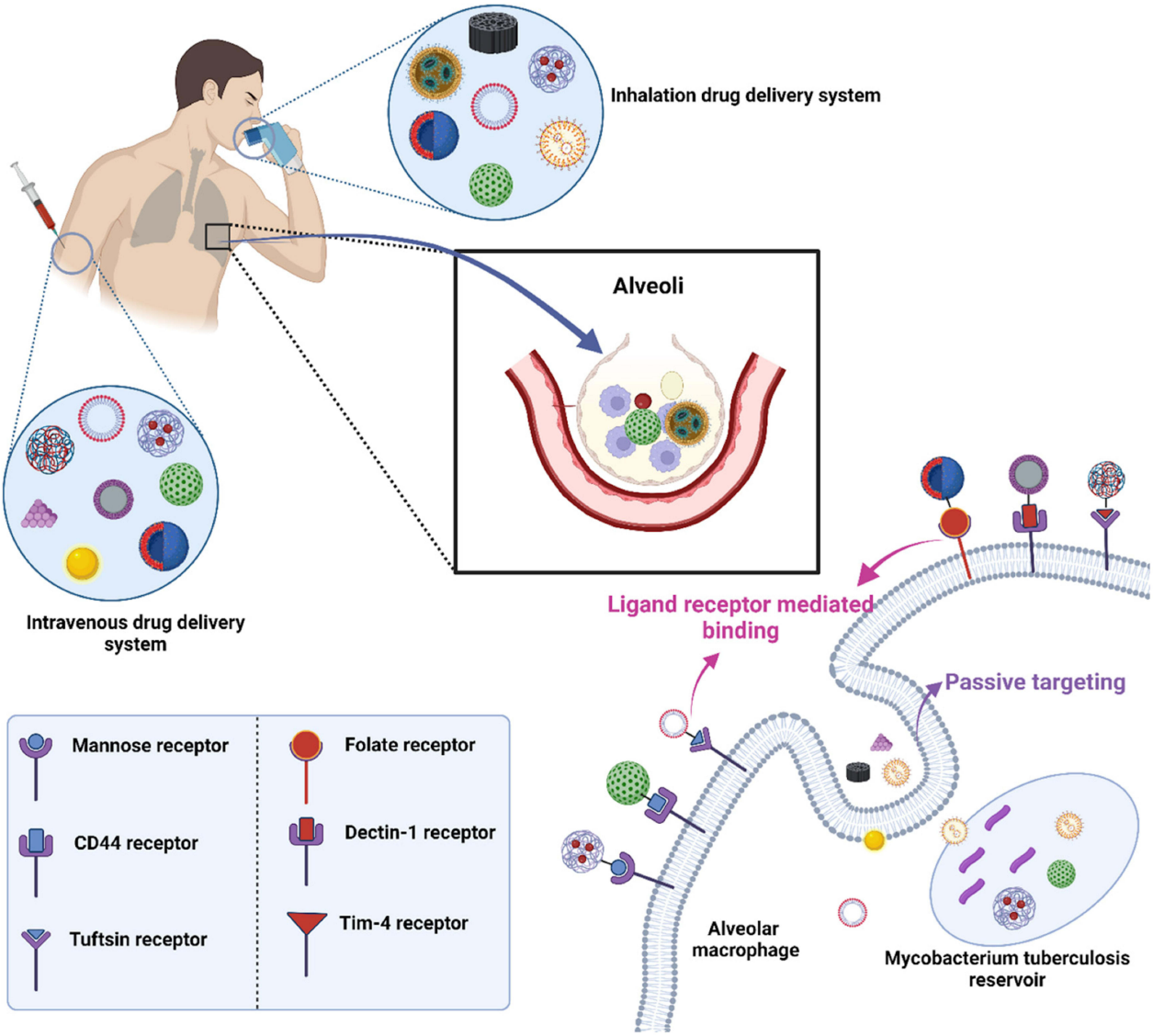

Figure 5 Ligand-receptor binding improves direct access to infected macrophage.[25]

mediated endocytosis also facilitates intracellular drug release.[133] However, protein ligands may face challenges such as immunogenicity and stability issues.[24]

Monoclonal Antibody and Aptamer

To achieve high specificity for TB biomarkers, Gilbride et al[31] developed an *M. bovis* monoclonal antibody as a surface modifier on NPs to target rMPT64. Bai et al[32] developed NPs functionalized with MPT64-binding aptamers to specifically target *Mtb* proteins, MPT64. Huang et al[33] developed NPs surface-modified with ESAT-6 antigen-binding aptamers for TB diagnostics. The study showed an aptamer coupling efficiency around 68%, which enhanced selective binding to ESAT-6 proteins on *Mtb*. These modification improved NP uptake in macrophage models with no significant reduction in cell viability.

Peptide

Li et al[48] developed ANG peptide as a surface modifier on NPs aimed at crossing biological barriers and targeting TB biomarker, H37Ra. They achieved over 15.8 ± 2.4% peptide conjugation efficiency, which correlated with increased uptake in macrophage-like cells. De Castro et al[49] used transferrin receptor (TfRs)-binding peptides to functionalize NPs

targeting macrophages. The peptide coupling efficiency was reported at 7.9%, facilitating a low amount of receptor-mediated endocytosis and enhanced NP uptake, with ~80% cell viability, demonstrating a significant biocompatibility.

Immunoglobulin

Churilov et al[50] developed single chain camel IgG as a surface modifier with coupling efficiency around 2.0 mg/g, which supported targeted delivery with increased macrophage uptake compared to non-modified controls. Cell viability remained high, confirming its safety.

Palmitoylated Tuftsin

Horváti et al[51] developed palmitoylated tuftsin as a surface modifier for TB-targeting NPs, which achieved a coupling efficiency around 90.5%, improving interaction with macrophage receptors and enhancing cellular uptake.

Macrophages

Macrophage-derived surface molecules as targeting moieties can more effectively recognize and bind to infected or activated macrophages. This macrophage-based targeting strategy exploits homotypic interactions and macrophage-specific markers to enhance selective uptake.[134] As a result, therapeutic agents are concentrated within diseased macrophage populations, improving treatment efficacy while minimizing off-target effects.[135]

Li et al[39] developed *M. marinum* stimulated macrophages as a surface modifier, enhancing therapeutic delivery to infected cells that significantly increased uptake compared to non-modified controls, as shown by quantitative fluorescence microscopy and flow cytometry analyses, with cell viability assays indicated low cytotoxicity.

Polymers

Polymers like PEG, pluronic block copolymers, and polyaniline are frequently employed as surface modifiers to enhance NP performance. PEGylation, in particular, provides a hydrophilic shield that minimizes opsonization and prolongs circulation time.[130] PEG helps keep NPs apart by surrounding them with a layer of water, which prevents them from sticking together, makes the NPs more stable in the body's fluids.[133] Functionalized polymers can also serve as conjugation platforms for targeting ligands.

Polyaniline

Chen et al[34] developed polyaniline as a surface modifier for biosensing applications, focusing on its conductive properties and functionalization efficiency. The study demonstrated successful immobilization of biomolecules onto polyaniline-coated surfaces and also showed promising results in detecting clinical PCR products.

Tetracycline-PEG

Liang et al[45] developed tetracycline-PEG conjugates as surface. Cellular uptake experiments using macrophage models revealed significantly enhanced internalization of TC-PEG-modified NPs compared to unmodified controls, attributed to the targeting capability of the TC moiety. Cell viability assays indicated that the TC-PEG conjugates were non-toxic up to relevant concentrations, having an approximately 100% cell viability, highlighting their potential for safe therapeutic delivery.

Carbohydrates

Carbohydrate-based surface modifiers can selectively bind to lectin-like receptors on immune cells, such as macrophages and dendritic cells.[133] For example, mannose-decorated NPs target the mannose receptor to enhance uptake by macrophages, while hyaluronic acid targets CD44-overexpressing cancer cells.[136] Carbohydrates are advantageous due to their low immunogenicity, ease of conjugation, and biodegradability.

Mannose

Maretti et al[36] developed methyl α-D-manno-pyranoside to modify NPs surface, to significantly enhance uptake by alveolar macrophages via mannose receptor targeting. Cell viability was under 80%, showing moderate biocompatibility. Maretti et al[37] developed mannose-modified SLNs showing increased lung accumulation, indicating effective targeting, though no quantitative coupling efficiency or uptake data were reported. Fan et al[40] developed mannose-modified

mesoporous polydopamine NPs (Man-mPDa), demonstrating improved therapeutic outcomes in mice without specifying coupling efficiency. Prabhu et al[47] developed mannose conjugation on chitosan NPs via FTIR, suggesting enhanced macrophage uptake, but lacked quantitative uptake or viability data. Pawde et al[52] developed mannose receptor-targeted bioadhesive chitosan, reporting increased cellular uptake, though coupling efficiency was not detailed. Maurya et al[53] developed a carubinose surface, a mannose analog, had a 15-fold uptake increase by macrophages measured by FACS, supporting strong targeting efficacy with cell viability of 61.14%. Vieira et al[55] developed mannosylated surface with enhanced macrophage uptake, with cell viability of ~95%. Lastly, Pinheiro et al[57] developed mannose surface modifier with 185.7 ± 253.7 mg/mL cell viability, indicating good biocompatibility and low cytotoxicity of the formulation.

N-Acetyl-D-Galactosamine 4-Sulfate

Mubin et al[41] developed 4-SO_4-GalNAc surface modifier. The study confirmed successful surface modification through specific binding assays, demonstrating effective coupling efficiency with no exact numerical values were not provided. Cellular uptake studies showed enhanced internalization of the modified NPs by macrophages compared to non-modified controls, and cytotoxicity assays indicated that the surface modification maintained high cell viability, supporting biocompatibility.

Alendronate

Garhyan et al[46] developed alendronate as a surface, reported enhanced cellular uptake by macrophages that observed through fluorescence microscopy and flow cytometry, confirming active targeting. Cell viability assays demonstrated minimal toxicity of the modified NPs at therapeutic doses, affirming their safety profile.

Curdlan Sulphate

Ravindran et al[58] developed curdlan sulphate as a surface modifier to facilitate macrophage targeting via Dectin-1 receptor binding with in vitro uptake studies demonstrated significantly higher internalization relative to unmodified particles. Cell viability tests showed no significant cytotoxicity, with numbers of 80% confirming the biocompatibility.

Hyaluronic Acid

Gao et al[60] developed HA surface modifier, leveraging the CD44 receptor. Coupling efficiency was confirmed qualitatively with cell viability of ~98%, indicating safe use in targeted therapies. Overall, while most studies confirm successful conjugation and enhanced internalization, quantitative coupling efficiency data vary or are limited.

Lipids

Lipids are commonly used to form or modify the surfaces of lipid-based nanocarriers to enhance membrane fusion and cellular uptake.[133] Amphiphilic lipids facilitate the integration of hydrophilic and hydrophobic components, aiding in encapsulation of a wide range of drugs. Moreover, lipid-modified surfaces can mimic biological membranes, improving biocompatibility and interaction with cellular lipid bilayers, although stability and oxidation may present formulation challenges.[137]

Mycolic Acid

Lemmer et al[62] developed mycolic acids as a surface modifier with uptake levels approximately 3-fold higher compared to non-modified NPs, as quantified by fluorescence assays. The mycolic acid coating facilitated increased interaction with macrophage membranes, likely due to the lipid's mimicry of mycobacterial cell wall components, which enhanced receptor-mediated endocytosis without significant toxicity.

Vitamin

Vitamins, particularly folic acid (vitamin B9), are effective small-molecule targeting ligands for NP surface modification. Folic acid binds with high affinity to folate receptors, which are overexpressed in many cancer types and activated macrophages, allowing for selective cellular uptake. Due to their small size, vitamins are easily conjugated to NP surfaces without significantly altering size or stability. Their low immunogenicity and natural biological roles make them more preferable, especially in systems requiring minimal toxicity and immune activation.[138]

Folic Acid

Choi et al[56] developed folic acid as a surface modifier to functionalize polymeric NPs for targeting folate receptor-overexpressing cells with cellular uptake studies showed that folic acid-modified NPs were internalized 4 to 5 times more efficiently by folate receptor-positive cells compared to unmodified controls, as evidenced by flow cytometry and confocal microscopy. Cell viability remained approximately 100% across tested concentrations, indicating minimal cytotoxicity.

Quantum Dots

Quantum dots (QDs) are semiconductor nanocrystals often used as diagnostic or imaging agents in theranostic nanocarriers.[139] QDs offer high fluorescence stability and tunable emission spectra, enabling real-time tracking of NP biodistribution and cellular uptake.[140] While not typically used as targeting ligands themselves, QDs can be co-functionalized with targeting moieties to enable simultaneous therapy and imaging.[141] However, concerns over heavy metal content[142] and long-term biocompatibility[143] must be addressed in clinical applications.

Cadmium Selenide/Zinc Sulfide Core-Shell

Bakhori et al[35] developed CdSe/ZnS QDs as fluorescent surface modifiers to enable imaging and tracking in biomedical applications, which was confirmed by photoluminescence spectroscopy showing strong and stable fluorescence emission characteristic of QDs. This successful surface modification allowed the NPs to retain their optical properties, essential for bioimaging purposes. Cellular uptake studies demonstrated that QD-modified NPs were efficiently internalized by target cells, as evidenced by flow cytometry and confocal microscopy analyses. The fluorescent signal from the QDs allowed clear visualization of intracellular NP localization, confirming effective uptake and intracellular distribution predominantly in the cytoplasm. MTT assays showed that QD surface modification did not induce significant cytotoxicity at relevant concentrations.

Functional Dye

Functional dyes, particularly pH- or redox-sensitive fluorophores, are employed on NP surfaces to monitor microenvironmental changes or release events.[144] Acid-sensitive dyes, for instance, fluoresce in response to endosomal or lysosomal pH, allowing for tracking of intracellular trafficking and drug release.[145] These dyes provide critical data for evaluating NP performance and can also be integrated into drug release mechanisms in stimuli-responsive systems.[146] For example, a recent study utilized an acid-sensitive fluorophore on a micellar nanocarrier for vaccine delivery, revealing strong fluorescence localized within acidic endosomes, providing direct visual evidence of successful cellular uptake and trafficking to the target compartment.[147]

Acid-Sensitive Fluorophore

Shang et al[44] developed an acid-sensitive fluorophore derived from a vitamin-based compound to serve as a surface modifier for targeted delivery and intracellular imaging. Successful surface conjugation was confirmed through fluorescence spectroscopy and pH-responsive fluorescence activation, demonstrating that the fluorophore remained functional after attachment to the NP surface. Cellular uptake studies showed enhanced internalization of these fluorophore-modified NPs in immune cells. Flow cytometry analyses further quantified increased NP uptake compared to non-modified controls. Additionally, cell viability assays confirmed that the fluorophore modification did not induce significant cytotoxic effects.

Combination

Combination strategies involve the simultaneous use of multiple surface modifiers to achieve synergistic targeting and therapeutic outcomes. For example, NPs may be PEGylated for extended circulation, functionalized with a ligand like folic acid for receptor-specific targeting, and tagged with a dye for imaging. Such multifunctional systems can overcome limitations of single-modifier approaches by enhancing targeting accuracy, improving pharmacokinetics, and enabling real-time monitoring.[38,42,43,54,59,61]

Mukhtar et al[38] developed a combination of mannosylated chitosan and HA to enhance targeting toward macrophages and CD44-expressing cells, with cellular uptake demonstrated significantly higher internalization of these dual-modified

NPs compared to single-ligand or unmodified controls, supporting synergistic targeting effects. Cell viability of ~90% assays indicated low cytotoxicity. Singh et al[42] developed PEGylation alongside thioaptamers for surface modification aimed at enhancing circulation time and targeting specificity, which showed increased cellular uptake in target cells via aptamer-mediated recognition, with flow cytometry revealing a 3-fold uptake increase relative to controls and cytotoxicity assays confirmed minimal toxicity. Gong et al[43] developed GalNAc and the immunomodulatory agent SR717 as surface modifiers, and enhanced uptake was observed in hepatocyte cell lines through receptor-mediated endocytosis, with confocal imaging showing co-localization of NPs in endosomal compartments. Liao et al[54] developed the combination of tuftsin and HA as dual surface modifiers on NPs targeting macrophages and CD44-positive cells with cellular uptake assays showed significantly enhanced NP internalization in infected cells compared to single modifications, indicating synergistic targeting, with cell viability assays demonstrated negligible cytotoxicity. Horváti et al[59] developed Pluronic F127 and tuftsin as surface modifiers with enhanced cellular uptake was observed in J774A.1 macrophages, with flow cytometry showing increased NP internalization relative to controls, the combined modification maintained high cell viability. Lastly, Tukulula et al[61] developed NPs functionalized with 1,3-β-glucan and rhodamine for targeted delivery and fluorescent tracking with enhanced uptake by macrophages was demonstrated through fluorescence microscopy and flow cytometry, showing strong internalization and intracellular localization and cell viability assays indicated low toxicity.

Discussion

Overall, a critical analysis of surface modifiers reveals a clear trend toward rational ligand design, where the choice of modifier is explicitly matched to overexpressed receptors on target cells, most notably macrophage-associated receptors like the mannose receptors and CD44. Carbohydrate like mannose and hyaluronic acid are frequently employed due to their low immunogenicity and high affinity for these receptors. In contrast, protein-based ligands such as antibodies and peptide offer high specificity but carry a greater risk of immunogenicity. An emerging narrative is the use of combination strategy to achieve both prolonged circulation and target specificity.

However, the field is limited by a lack of standardized quantification for ligand coupling efficiency, a critical source of heterogeneity that makes it difficult to compare the true efficacy of different targeting strategies. While most studies confirm successful conjugation and enhanced cellular uptake, the absence of quantitative data prevents a clear conclusion in which modification strategy is superior. This highlights a need for more rigorous quantitative reporting in future studies.

Pharmaceutical Dosage Forms for Active Targeting Nanoparticles Delivery Systems

In TB management, pharmaceutical dosage forms for active targeting NP systems vary depending on the clinical purpose via different delivery routes.[18] Each use case demands a form that preserves the integrity and function of the targeting component while optimizing delivery to infected or immune-relevant sites (Figure 6). In the context of diagnostic applications, actively targeted NPs are increasingly incorporated into biosensor platforms or contrast agents.[148] These diagnostic forms are typically formulated as ready-to-use suspensions[31,32] or immobilized on paper or chip-based devices.[33–35] For therapeutic applications, especially in pulmonary TB, inhalable dosage forms dominate due to their direct access to alveolar macrophages. Dry powder inhalers (DPIs), nebulized suspensions, and metered dose inhalers are commonly employed to deliver ligand-functionalized NPs.[36–38] For systemic or extrapulmonary TB, parenteral dosage forms are used to deliver NPs conjugated with antibodies or peptides that target infected tissues with specific receptors.[149] For PPT, especially in high-risk populations or latent TB infection, long-acting injectable NPs are being explored.[39,40] In vaccine delivery, NP-based carriers are increasingly formulated into intramuscular[150] or mucosal[151] vaccines to enhance antigen presentation.

Diagnostic Tool

Gilbride et al[31] developed Au–Fe_3O_4 NP-antibody bioconjugates targeting rMPT64. The assay achieved a LOD_{50} of 147 CFU/mL and an EC_{50} of 198.7 ng/mL, indicating sensitivity to low bacterial concentrations. The peroxidase-mimicking

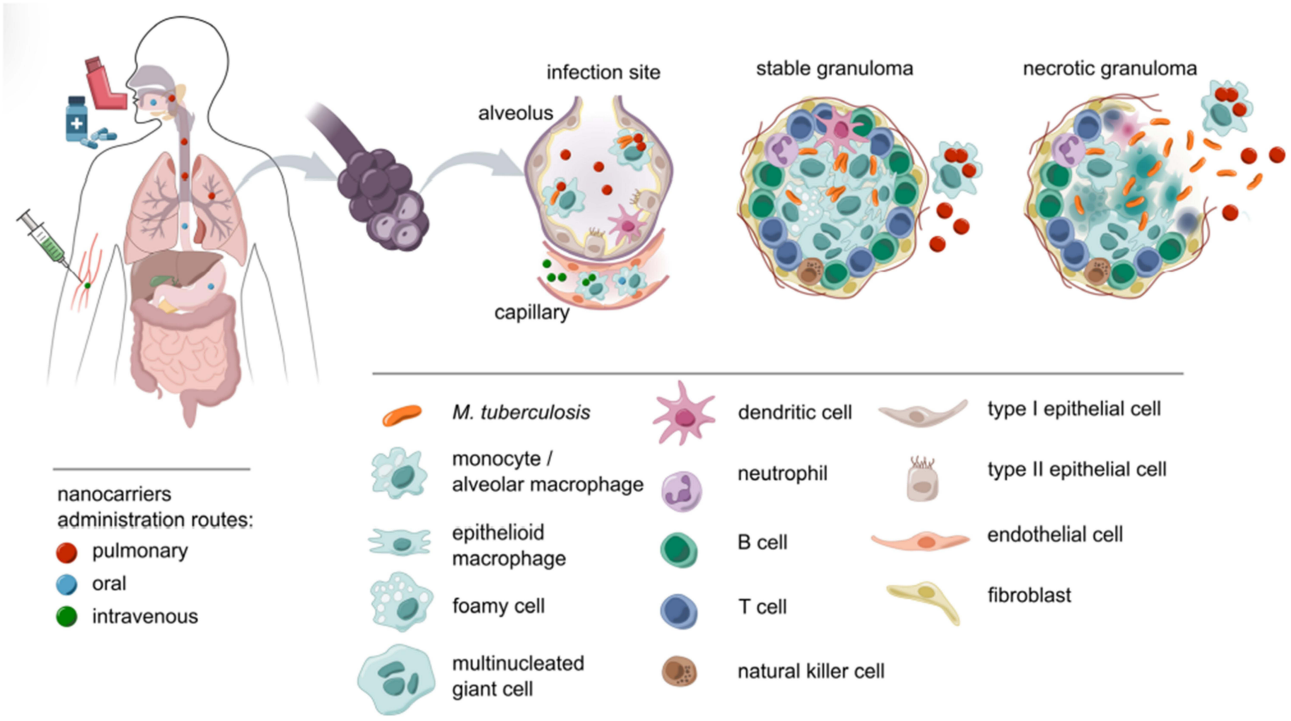

Figure 6 Different delivery routes of nanoparticles to infected sites.[152]

activity of the Au–Fe_3O_4 NPs facilitated rapid signal generation, reaching approximately 81% activity within 10 minutes. This platform combines magnetic separation and visible color change in a single NP, offering simplicity and rapid results. Bai et al[32] developed GNPs-C_{60}-PAn NPs for detecting MPT64 antigen. The sensor demonstrated a remarkably low LOD of 20 fg/mL and a calculated antigen value of 0.9728 pg/mL, showcasing ultrahigh sensitivity with %RSD of 6.3% and recovery rate of 97.28% confirms high analytical accuracy. Huang et al[33] developed MXene/C_{60}NPs/Au@Pt hybrids targeting ESAT-6, achieving an low LOD of 2.88 fg/mL and a calculated antigen concentration of 0.982 ng/mL. The low %RSD of 1.9% reflects high precision, and the recovery rate of 98.2% supports the system's analytical validity. They also demonstrated dual independent signal outputs, one from fullerene redox activity and one from Au@Pt electrocatalysis, and achieved 97.5% sensitivity and 96.7% specificity when comparing samples from TB patients, healthy donors, and individuals with other lung diseases. Chen et al[34] developed Au–CNTs–PAn DNA biosensor for the IS6110 genetic sequence, achieved a LOD of 0.33 fM, indicating high and %RSD of 3.17% confirms acceptable reproducibility. The unique flower-like structure of the CNTs-PAN nanohybrid contributed to the sensor's large surface area and efficient redox activity, enhancing signal transduction. Bakhori et al[35] developed CdSe/ZnS QDs and silica NPs on a SPCE to detect the CFP10–ESAT6 antigen, achieved a LOD of 1.5×10^{-10} g/mL and exhibited a peroxidase activity of approximately 22% at 100 ng/mL. The %RSD of 1.45% indicates high reproducibility. The use of QD enhanced the electrochemical signal, improving sensitivity.

Overall, these NP-based biosensors summarized in Table 3, exhibit strong potential as advanced diagnostic tools for TB, significantly outperforming many conventional detection methods. Compared to traditional TB diagnostics like sputum smear microscopy or culture, which suffer from low sensitivity, long turnaround times, and dependence on viable bacterial load, these nanosensors offer rapid detection with excellent reproducibility and minimal sample requirements.

Photothermal Therapy

Li et al[39] developed BBTD@PM NPs, upon NIR-II irradiation at 1,064 nm with power density of 0.2 W/cm^2, the NPs achieved a peak intrapulmonary temperature of ~55°C. In vitro treatment of H37Ra bacilli yielded complete bacterial clearance with ~0 CFU/mL, and in vivo imaging showed markedly higher accumulation of NIR-IIb fluorescence in lung

https://doi.org/10.2147/IJN.S557784

Table 3 Analytical Performance of Actively Targeted TB Immune Detection Assay Nanoparticles

NPs Name	TB Biomarker	Calculated Antigen	LOD/LOD_{50}	EC_{50}	Peroxidase Activity	RSD	Recovery	Authors
Au–Fe3O4 NP-antibody bioconjugates	rMPT64	NA	LOD_{50} = 147 CFU mL^{-1}	198.7 ng/mL	~81% after 10 min	NA	NA	[31]
GNPs-C60-PAn	MPT64	0.9728 pg/mL	LOD = 20 fg/mL	NA	NA	6.3%	97.28%	[32]
MXene/C60NPs/Au@Pt	ESAT-6	0.982 ng/mL	LOD = 2.88 fg/mL	NA	NA	1.9%	98.2%	[33]
Au-CNTs-PAN	IS6110	NA	LOD = 0.33 fM	NA	NA	3.17%	NA	[34]
CdSe/ZnS QD/SiNPs/SPCE	CFP10-ESAT6	NA	LOD = 1.5×10^{-10} g/mL	NA	~22% at 100 ng/mL	1.45%	NA	[35]

Abbreviations: NPs, Nanoparticles; TB, Tuberculosis; LOD, Limit of detection; LOD_{50}, Limit of detection at 50%; EC_{50}, Half maximal effective concentration; RSD, Relative standard deviation; rMPT64, Recombinant *Mycobacterium tuberculosis* protein 64; CFU, Colony-forming units; MPT64, *Mycobacterium tuberculosis* protein 64; ESAT-6, Early secreted antigenic target 6 kDa; IS6110, Insertion sequence 6110; CFP10, Culture filtrate protein 10 kDa; NA, Not available.

tissue compared to uncoated NPs with biotoxicity assessment revealed minimal adverse effects. As a theragnostic agent, BBTD@PM also allowed real-time tracking of localization and thermal activation, demonstrating both therapeutic and diagnostic capabilities seamlessly integrated into a single delivery system. Fan et al[40] developed Rif@Man-mPDA under 808 nm NIR light at 1.2 W/cm^2, the particles heated to 51.3°C, reducing H37Ra bacterial counts to ~5×10^3 CFU/mL, indicating significant but incomplete clearance. In a cutaneous TB mouse model, the NPs generated strong NIR signals in skin lesions with the treatment significantly reduced both extracellular and intracellular bacterial loads in macrophages.

Overall, these actively targeted PTT systems summarized in Table 4, demonstrate superior precision therapy by achieving high local temperatures under mild irradiation, effectively reducing bacterial load, and allowing non-invasive imaging-guided therapy, they offer improved treatment accuracy, reduced tissue damage, and the ability to monitor biodistribution, marking a significant leap beyond traditional PTT approaches.

Vaccine

Mubin et al[41] developed CNP-L chitosan NPs, these particles inhibited more than 60% of *Mtb* biofilm formation at a concentration of 100 µg/mL and significantly reduced bacterial burden to ~3,500 CFU/mL. Importantly, the system activated antigen-specific T-cells effectively, suggesting its effectiveness in delivering vaccine payloads to infected cells and initiating an antibacterial immune reaction. Singh et al[42] developed CD44TA-LIP, in TB-infected mice, intranasal immunization reduced lung bacterial loads to about 4.8 log_{10} CFU. The formulation robustly activated antigen-specific T cells and memory T cell subsets, with increased levels of interferon-γ, IL-2, and TNF-α, as well as elevated populations of effector, central, and resident memory CD4+ and CD8+ T cells. These results highlight CD44TA-LIP's ability to provide broad and long-lasting protective immunity as a vaccine. Gong et al[43] developed TP/GPS NPs, in TB-infected mice where bacterial loads decreased to 6.0 log_{10} CFU. TP/GPS induced strong activation of antigen-specific T cells and enhanced proliferation of long-lived CD4+ and CD8+ memory T cells. The particles also promoted sustained expression of granzyme B and interferon-γ in CD8+ T cells, confirming their ability to be durable and immune protective. Shang et al[44] developed PEG-PPS with release and bacterial burden data were not reported, the vaccine showed highly effective activation of both antigen-specific and memory T-cells in vivo, indicating a strong and lasting immune response. The

Table 4 Analytical Performance of Actively Targeted TB Photothermal Therapy Nanoparticles

NPs Name	TB Biomarker	NIR Irradiation	Maximum Temperature	In vitro CFU	Imaging Model	NIR-IIb Signals	Biotoxicity	Authors
BBTD@PM	H37Ra	0.2 w/cm^2 1,064 nm	~55°C	~0 × 10^6 CFU/mL	TB mice	Higher in lung tissues	Low	[39]
Rif@Man-mPDA	H37Ra	1.2 w/cm^2 808 nm	51.3°C	~5,000 CFU/mL	CTB mice	Higher in skin tissues	Low	[40]

Abbreviations: NPs, Nanoparticles; TB, Tuberculosis; NIR, Near-infrared; CFU, Colony-forming units; NIR-IIb, Near-infrared IIb; CTB, Cutaneous tuberculosis.

ASF peptide on the micelle surface promoted antigen targeting, a key design component for maximizing immune engagement.

Overall, these actively targeted NP-based vaccines summarized in Table 5, unlike traditional formulations, they incorporate surface ligands or immune-targeting motifs that enable precise delivery to immune cells, enhancing antigen presentation and T-cell activation. Thus, these actively targeted vaccines represent a significant advancement toward more effective, durable, and site-specific immunization strategies for TB.

Inhalation Treatment

Maretti et al[36] developed RIF-SLNas with excellent aerodynamic characteristics with a fine particle fraction (FPF) below 4.46 µm, an emitted dose (ED) of 97.65%, and a good angle of repose of 29.18°, indicating good flowability. Wettability was measured at 47.38°, which supports efficient dispersion in lung fluids, with 100% cell viability after 3 hours at 0.25 mg/mL, demonstrating its safety for lung epithelial cells. Maretti et al[37] developed SLNas/MS with a FPF under 6 µm and an ED of 87%, the formulation demonstrated effective aerodynamic performance. The mannosylation improved targeting to alveolar macrophages via mannose receptors, and the NPs showed good dispersibility with wettability of 51°, the system maintained ~80% cell viability at 0.25 mg/mL after 6 hours, indicating a good safety profile, with prolonged RIF retention in macrophages and improved uptake. Mukhtar et al[38] developed INH-MC/HA, which showed strong performance in pulmonary delivery, with an FPF of 35% and an aerodynamic diameter below 3 µm, suitable for alveolar deposition. In vitro cytotoxicity assays showed ~90% cell viability even after 24 hours at a low dose of 0.01 mg/mL, confirming excellent biocompatibility.

Overall, these inhalable NP-based formulations as summarized in Table 6, significantly improved wettability and powder flow, higher emitted dose, and fine particle fractions enhance deposition in the deep lung, with the addition of targeting moieties enabling selective delivery to infected cells, increasing therapeutic concentration at the infection site. High levels of cell viability across all studies also affirm the safety of these systems for respiratory delivery, offering greater precision and reduced systemic exposure.

Standard Treatment

Liang et al[45] developed a RPT co-loaded TC–PLGA–PEG NPs that achieved MIC of 0.094 µg/mL with a cell viability of ~100%, highlighting excellent biocompatibility and a highly effective and safe system for TB treatment. Garhyan et al[46] developed INH and RIF loaded BTL NPs that achieved reduced intracellular CFU count of ~9×10^7 CFU/cells in THP-1 cells, indicating improved drug delivery and intracellular killing potential. Prabhu et al[47] developed RIF-loaded MCNPs that achieved an exceptionally low MIC of 0.009 µg/mL, supporting strong anti-TB efficacy. Li et al[48] developed ANG-Exo-RIF which achieved high cell compatibility of ~98% viability at 0.25 µg/mL and equal MIC and MBC values of 0.25 µg/mL, signifying effective bactericidal activity, confirming its dual role as a potent and safe formulation for

Table 5 Analytical Performance of Actively Targeted TB Vaccines Nanoparticles

NPs Name	EE/DL	In vitro Release	Biofilm Inhibition	Immunized Model	CFU	Activated Ag-Specific T-Cells	Activated Memory T-Cells	Authors
CNP-L	DL = 79%	70% after 12–14h	> 60% with 100 µg/mL	NA	In vitro = ~3,500 CFU/mL	Effective	NA	[41]
CD44TA-LIP	NA	NA	NA	Mice	In vivo = ~4.8 $\log_{10}$ CFU	Highly effective	Highly effective	[42]
TP/GPS	EE = 62.7% DL = 2.5%	NA	NA	Mice induced H37Ra	In vivo = 6.0 $\log_{10}$ CFU	Highly effective	Highly effective	[43]
MA-loaded Micelle PEG-PPS-ASF	DL = 92 ± 3%	NA	NA	Mice induced DN1 T-cells	NA	Highly effective	Highly effective	[44]

Abbreviations: NPs, Nanoparticles; EE, Encapsulation efficiency; DL, Drug loading; CFU, Colony-forming units; DN1 T-cells, Double negative 1 T-cells; NA, Not available.

https://doi.org/10.2147/IJN.S557784

Table 6 Analytical Performance of Actively Targeted TB Inhalation Treatment Nanoparticles

NPs Name	EE	DL	Wettability	Angle of Repose	FPF	ED	Cell Viability	Authors
RIF-SLNas	43.60 ± 1.86%	14.53 ± 0.62%	47.38 ± 6.91°	29.18 ± 2.20°	< 4.46 μm	97.65 ± 0.15%	100% at 0.25 mg/mL in 3h	[36]
SLNas/MS	36.8 ± 0.9%	9.2 ± 0.2%	51°	NA	38 ± 5% < 6 μm	87 ± 4%	~80% at 0.25 mg/mL after 6h	[37]
INH-MC/HA	92.31 ± 2.06%	25.9 ± 2.11%	NA	NA	35% < 3 μm	NA	~90% at 0.01 mg/mL after 24h	[38]

Abbreviations: NPs, Nanoparticles; EE, Encapsulation efficiency; DL, Drug loading; FPF, Fine particle fraction; ED, Emitted dose; NA, Not available.

targeted delivery to brain lesions in TB meningitis. De Castro et al[49] developed their NP-CFZ NPs, which achieved ~80% viability at 1 μM over 24 hours, supporting its good safety. Horváti et al[51] developed PLGA-pT820 NPs with a high MIC of 10 mg/mL, suggesting moderate potency, while their later work, Horváti et al[59] that developed TB515-PLGA-T10Tp showed remarkable efficacy with bacterial counts dropping to ~1 CFU per sample. Both studies underline the role of peptide-modified PLGA in antimicrobial targeting. Maurya et al[53] developed LVF-CHF that achieved 61.14% cell viability at 50 ppm after 72 hours, reflecting good tolerability. Gao et al[60] developed RIF-HA-TS7 NPs that achieved ~98% viability at 0.01 mg/mL and increased proinflammatory cytokine responses, suggesting strong immune activation as a treatment. Liao et al[54] developed Tuf-Rif@HA-MnO_2, which significantly reduced bacterial load by ~3.6 $\log_{10}$ CFU/well and enhanced proinflammatory cytokine production, indicating strong immunomodulatory effects alongside therapeutic action. Ravindran et al[58] developed CSC: D-PIN + RIF that also significantly reduced CFU by ~10^3 CFU/mL with increased proinflammatory cytokine expression and an MIC of 6.37 ± 2.04 μg/mL, indicating strong antibacterial activity and is capable of stimulating the host immune response. Vieira et al[55] developed M-NLCs-RIF, which achieved ~95% cell viability at 100 μg/mL and reducing CFU by ~1.5 $\log_{10}$ CFU/mL, confirming its potential for macrophage-targeted TB therapy. Pinheiro et al[57] developed M-NLC-RFB was similarly safe, with 185.7 ± 253.7 mg/mL viability observed. Choi et al[56] developed GaF formulation that achieved near-total bacterial killing of ~100% viability at 0.5 mM and significant CFU reduction of ~30×10^4 CFU/mL, indicating strong antimicrobial action, demonstrating gallium's role as a promising metal-based TB agent.

Although some studies demonstrated potential through their respective NP formulations, even though certain parameters like CFU reduction or MIC were not reported, the active targeting NP formulations summarized in Table 7, demonstrate enhanced cell viability, and potent bacterial reduction compared to traditional TB therapies. Their additional sustained release allows for prolonged drug presence at the site of infection, reducing dosing frequency and potentially improving patient compliance. Additionally, several formulations show immunomodulatory effects through increased proinflammatory cytokine production, compared to conventional treatment, making them superior candidates for the next generation of TB standard treatments.

Discussion

Overall, the studies underscore that the pharmaceutical dosage form is not an afterthought but a critical component tailored to the specific application, whether it be diagnostics, therapy, or vaccination. For pulmonary TB, inhalable dosage form DPIs are logically favored to deliver drugs directly to alveolar macrophages. In contrast, systemic or extrapulmonary TB necessitates parenteral forms to reach disseminated infection sites.

A critical comparison of the PPT studies reveals a key source of heterogeneity. Li et al[39] achieved complete bacterial clearance (~0 CFU/mL), while Fan et al[40] reported only partial clearance (~5,000 CFU/mL). This difference is likely attributable to the distinct NIR irradiation parameters used (1,064 nm at 0.2 W/cm^2 vs 808 nm at 1.2 W/cm^2), highlighting how technical specifics can alter outcomes. Similarly, the vaccine studies show promise but use varied animal models, making direct comparison of CFU reduction challenging. The diagnostics tools consistently demonstrate a major leap in performance, with LOD in femtogram (fg/mL) range, orders of magnitude more sensitive than traditional methods.

Table 7 Analytical Performance of Actively Targeted Various TB Treatment Nanoparticles

NPs Name	EE	DL	Drug Release	Cell Viability	CFU	MIC/MBC	Cytokine Production	Authors
RPT/TC–PLGA–PEG	83.3 ± 5.5%	8.1 ± 0.4%	90% in 6h	~100%	NA	MIC = 0.094 μg/mL	NA	[45]
INH BTL	69.5 ± 4.2%	NA	~80% in 70h	NA	~9×10^7 CFU/cells	NA	NA	[46]
RIF BTL	70.6 ± 4.7%		~70% in 70h					
Rifampicin MCNPs	70.86%	NA	70.3% in 40h	NA	NA	MIC = 0.009 μg/mL	NA	[47]
ANG-Exo-RIF	18.8 ± 2.4%	NA	NA	~98% at 0.25 μg/mL	NA	MIC = 0.25 μg/mL MBC = 0.25 μg/mL	NA	[48]
NP-CFZ5% Mal20%: Pep	63.38 ± 7.76%	3.33 ± 0.41%	NA	~80% at 1 μM in 24h	NA	NA	NA	[49]
PCZ-PLA	32%	NA	~30% in 15h	NA	NA	NA	NA	[50]
PLGA-pT820	83%	20.2%	NA	NA	NA	MIC = 10 mg/mL	NA	[51]
Cfz-CS-MNS-NP	73.45 ± 1.47%	NA	70.98% in 72h	NA	NA	NA	NA	[52]
LVF-CHF	64.36%	15.46 ± 0.33%	~80% in 72h	61.14% at 50 ppm	NA	NA	NA	[53]
Tuf-Rif@HA-MnO_2	NA	NA	NA	NA	~3.6 $\log_{10}$ CFU/well	NA	Increased proinflammatory	[54]
M-NLCs-RIF	95 ± 2%	1.3 ± 0.1%	~20% in 3h	~95% at 100 μg/mL in 24h	~1.5 $\log_{10}$ CFU/mL	NA	NA	[55]
GaF	NA	NA	NA	~100% at 0.5 mM	~30×10^4 CFU/mL	NA	NA	[56]
M-NLC-RFB	90 ± 4%	NA	100% in 25h	185.7 ± 253.7 mg/mL	NA	NA	NA	[57]
CSC: D-PIN + RIF	NA	245 μg/mg	65% in 48h	80% at 100 μg/mL in 48h	~10×10^3 CFU/mL	MIC = 6.37 ± 2.04 μg/mL	Increased proinflammatory	[58]
TB515-PLGA-T10Tp	NA	3.5%	NA	NA	~1 CFU	NA	NA	[59]
RIF-HA-TS_7	NA	70.01 ± 0.85%	79.82% in 13h	~98% at 0.01 mg/mL	NA	NA	Increased proinflammatory	[60]
Glu-PLGA-Rh (RIF)	NA	1.1 ± 0.1 μg/mg	~10% in 24h	NA	NA	NA	NA	[61]
PLGA/INH/MA	42%	5%	NA	NA	NA	NA	NA	[62]

Abbreviations: NPs, Nanoparticles; EE, Encapsulation efficiency; DL, Drug loading; CFU, Colony-forming units; MIC, Minimum inhibitory concentration; MBC, Minimum bactericidal concentration; ppm, Parts per million; NA, Not available.

Limitations and Future Prospects

A critical assessment of the studies included in this review reveals several key limitations. The most significant is the predominance of preclinical models. The vast majority of the mice models use in PTT findings presented are derived from in vitro cell cultures and in vivo animal studies, such as the mice models use biocompatibility and high cell viability in PTT and vaccine evaluation. While essential for initial proof-of-concept, there is a clear lack of data from human clinical trials, which is the crucial step for validating both safety and efficacy of these complex systems. Furthermore, a recurring limitation across the studies is the inconsistent reporting of key parameters of NPs characteristics.

Beyond the limitations of the existing studies, scalability is a primary concern, as transition from small-scale synthesis to consistent, large-scale good manufacturing practice is a complex challenge. Nanomedicines also face stringent regulatory hurdles, requiring extensive characterization and data on long-term toxicity. While many studies confirm good short-term biocompatibility and high cell viability, the long-term fate and potential for organ accumulation of these nanomaterials are largely unknown and are critical concerns for a chronic illness like TB. Finally, the cost of these advanced therapies, which often involve complex synthesis and expensive targeting ligands, could pose a barrier to their widespread adoption, particularly in the high-burden settings where novel TB treatments are needed the most.

Conclusion

Actively targeted nanoparticles offer a promising strategy to overcome long-standing limitations in TB management, including poor drug bioavailability, systemic toxicity, and the emergence of drug resistance. By enabling selective delivery to infected sites, enhancing diagnostic accuracy, and improving therapeutic response, these nanoformulations provide a more efficient and patient-adapted approach to TB care. However, it is crucial to acknowledge that the field is still in its early stages. Significant hurdles must be addressed. Therefore, while the future of actively targeted nanomedicine is bright, rigorous and concerted research efforts are essential to bridge the gap between laboratory innovation and clinical reality, ultimately contributing to global disease control and eradication.

Abbreviation

Acr-1, Alpha-crystallin-1 antigen; Ag-specific, Antigen-specific; AIE, Aggregation-induced emission; AMs, Alveolar macrophages; ANG, Angiopep-2; APCs, Antigen-presenting cells; ASGPRs, Asialoglycoprotein receptors; ASF, Acid-sensitive fluorophore; BBBs, Blood–brain barriers; BCS, Biopharmaceutics classification system; BECs, Brain endothelial cells; BPaL, Bedaquiline, Pretomanid, and Linezolid; CD1b, Cluster of differentiation 1b; CD44, Cluster of differentiation 44; CFP10, Culture filtrate protein 10 kDa; CFU, Colony-forming units; CFZ, Clofazimine; CHF, Chitosan hydrogel formulation; CLRs, C-type lectin receptors; CNS-TB, Central nervous system tuberculosis; CNTs, Carbon nanotubes; CS, Chitosan; CSC, Curdlan sulphate-chitosan; CTB, Cutaneous tuberculosis; DCs, Dendritic cells; DDS, Drug delivery system; Dectin-1, Dendritic cell-associated C-type lectin-1; DL, Drug loading; DN1, Double negative 1; dUTPase, Deoxyuridine triphosphatase; EC_{50}, Half maximal effective concentration; ED, Emitted dose; EE, Encapsulation efficiency; EPTB, Extrapulmonary tuberculosis; ESAT-6, Early secreted antigenic target 6 kDa; Exo, Exosomes; FPF, Fine particle fraction; GalNAc, N-Acetylgalactosamine; HA, Hyaluronic acid; HRZE, Isoniazid, Rifampicin, Pyrazinamide, and Ethambutol; IgG, Immunoglobulin G; INH, Isoniazid; IS6110, Insertion sequence 6110; LIP, Liposome; LOD, Limit of detection; LOD_{50}, Limit of detection at 50%; LVX, Levofloxacin; MA, Mycolic acids; MAC, *M. avium* complex; Man, Mannose; MBC, Minimum bactericidal concentration; MCNPs, Mesoporous carbon nanoparticles; MDR-TB, Multidrug-resistant tuberculosis; MDMs, Monocyte-derived macrophages; MHC, Major histocompatibility complex; MIC, Minimum inhibitory concentration; MNPs, Metallic-based nanoparticles; MNS, Mesoporous nanostructured silica; mPDA, mesoporous Polydopamine; MRs, Mannose receptors; MS, Microspheres; *Mtb, Mycobacterium tuberculosis*; MTBC, *Mycobacterium tuberculosis* complex; MPT64, *Mycobacterium tuberculosis* protein 64; MXene, A class of 2D inorganic compounds; NA, Not available; NEs, Nanoemulsions; NIR, Near-infrared; NIR-IIb, Near-infrared IIb; NLCs, Nanostructured lipid carriers; NP, Nanoparticle; PCZ, Perchlozone©; PCR, Polymerase chain reaction; PDI, Polydispersity index; PEG, Polyethylene glycol; Pep, Peptide; PLA, Polylactic acid; PLGA, Poly(lactic-co-glycolic) acid; PNPs, Polymeric nanoparticles; PPS, Poly(propylene sulfide); PTT, Photothermal

therapy; QDs, Quantum dots; RFB, Rifabutin; RIF, Rifampicin; rMPT64, Recombinant *Mycobacterium tuberculosis* protein 64; RPT, Rifapentine; RSD, Relative standard deviation; SLNs, Solid lipid nanoparticles; SPCEs, Screen-printed carbon electrodes; TB, Tuberculosis; TC, Tetracycline; TfRs, Transferrin receptors; TLRs, Toll-like receptors; TPE-BT-BBTD, Tetraphenylethylene-benzothiadiazole-bis-benzothiadiazole; Tuf, Tuftsin; WHO, World Health Organization; XDR, Extensively drug-resistant.

Acknowledgment

This publication charge is funded by Universitas Padjadjaran through the Indonesian Endowment Fund for Education (LPDP) on behalf of the Indonesian Ministry of Higher Education, Science and Technology and managed under the EQUITY Program (Contract No. 4303/ B3/DT.03.08/2025 and 3927/UN6. RKT/HK.07.00/2025).

Disclosure

The authors declare that they have no known competing financial interests or personal relationships that could have appeared to influence the work reported in this paper.

References

1. Sinha P, Gupta A, Prakash P, Anupurba S, Tripathi R, Srivastava GN. Differentiation of Mycobacterium tuberculosis complex from non-tubercular mycobacteria by nested multiplex PCR targeting IS6110, MTP40 and 32kD alpha antigen encoding gene fragments. *BMC Infect Dis*. 2016;16(1):1–10. doi:10.1186/s12879-016-1450-1
2. WHO. Tuberculosis; 2025. Available from: https://www.who.int/news-room/fact-sheets/detail/tuberculosis. Accessed June 10, 2025.
3. Heye T, Stoijkovic M, Kauczor HU, Junghanss T, Hosch W. Extrapulmonale Tuberkulose: die radiologische Bildgebung eines fast vergessenen Verwandlungskünstlers. *RoFo Fortschritte auf dem Gebiet der Rontgenstrahlen und der Bildgebenden Verfahren*. 2011;183(11):1019–1029. doi:10.1055/S-0031-1273429
4. World Health Organization. *WHO Consolidated Guidelines on Tuberculosis: Module 4: Treatment - Drug-Susceptible Tuberculosis Treatment*. PMID: 35727905. Published online 2022. Geneva: World Health Organization;2022.
5. Borah Slater K, Kim D, Chand P, Xu Y, Shaikh H, Undale V. A current perspective on the potential of nanomedicine for anti-tuberculosis therapy. *Trop Med Infect Dis*. 2023;8(2):100. doi:10.3390/TROPICALMED8020100
6. Conradie F, Diacon AH, Ngubane N, et al. Treatment of highly drug-resistant pulmonary tuberculosis. *N Engl J Med*. 2020;382(10):893–902. doi:10.1056/NEJMOA1901814
7. Dartois V. The path of anti-tuberculosis drugs: from blood to lesions to mycobacterial cells. *Nat Rev Microbiol*. 2014;12(3):159–167. doi:10.1038/NRMICRO3200
8. Maiga M, Abaza A, Bishai WR. Current tuberculosis diagnostic tools & role of urease breath test. *Indian J Med Res*. 2012;135(5):731.
9. Gopalaswamy R, Shanmugam S, Mondal R, Subbian S. Of tuberculosis and non-tuberculous mycobacterial infections – a comparative analysis of epidemiology, diagnosis and treatment. *J Biomed Sci*. 2020;27(1):1–17. doi:10.1186/S12929-020-00667-6
10. Cole B, Nilsen DM, Will L, Etkind SC, Burgos M, Chorba T. Essential components of a public health tuberculosis prevention, control, and elimination program: recommendations of the advisory council for the elimination of tuberculosis and the national tuberculosis controllers association. *MMWR Recommendations Rep*. 2020;69(7):1. doi:10.15585/MMWR.RR6907A1
11. Magalhães J, Vieira A, Santos S, Pinheiro M, Reis S. Oral administration of nanoparticles-based TB drugs. *Multifun Syst Combined Deliv Biosens Diagnostics*. 2017:307–326. doi:10.1016/B978-0-323-52725-5.00016-2
12. Eddabra R, Ait Benhassou H. Rapid molecular assays for detection of tuberculosis. *Pneumonia*. 2018;10(1):1–12. doi:10.1186/S41479-018-0049-2
13. Aslan G. Diagnosing tuberculosis: traditional and new methods against an old enemy. *J Clin Pract Res*. 2024;46(5):431–443. doi:10.14744/cpr.2024.95839
14. Lee JY. Diagnosis and treatment of extrapulmonary tuberculosis. *Tuberc Respir Dis*. 2015;78(2):47–55. doi:10.4046/TRD.2015.78.2.47
15. Borandeh S, van Bochove B, Teotia A, Seppälä J. Polymeric drug delivery systems by additive manufacturing. *Adv Drug Deliv Rev*. 2021;173:349–373. doi:10.1016/J.ADDR.2021.03.022
16. Eltaib L. Polymeric nanoparticles in targeted drug delivery: unveiling the impact of polymer characterization and fabrication. *Polymers*. 2025;17(7):833. doi:10.3390/POLYM17070833
17. Kia P, Ruman U, Pratiwi AR, Hussein MZ. Innovative therapeutic approaches based on nanotechnology for the treatment and management of tuberculosis. *Int J Nanomed*. 2023;18:1159–1191. doi:10.2147/IJN.S364634
18. Pourakbari R, Shadjou N, Yousefi H, et al. Recent progress in nanomaterial-based electrochemical biosensors for pathogenic bacteria. *Mikrochim Acta*. 2019;186(12):1–13. doi:10.1007/s00604-019-3966-8
19. Golichenari B, Nosrati R, Farokhi-Fard A, Abnous K, Vaziri F, Behravan J. Nano-biosensing approaches on tuberculosis: defy of aptamers. *Biosens Bioelectron*. 2018;117:319–331. doi:10.1016/j.bios.2018.06.025
20. Muthukrishnan L. Multidrug resistant tuberculosis – diagnostic challenges and its conquering by nanotechnology approach – an overview. *Chem Biol Interact*. 2021;337. doi:10.1016/j.cbi.2021.109397
21. Dewangan P, Mourya A, Singh PK, et al. Drug delivery: the conceptual perspectives and therapeutic applications. *Polymer-Drug Conjugates*. 2023:1–38. doi:10.1016/B978-0-323-91663-9.00010-2
22. Hammood M, Craig AW, Leyton JV. Impact of endocytosis mechanisms for the receptors targeted by the currently approved antibody-drug conjugates (ADCs)—a necessity for future ADC research and development. *Pharmaceuticals*. 2021;14(7):674. doi:10.3390/PH14070674

23. Jiskoot W, Randolph TW, Volkin DB, et al. Protein instability and immunogenicity: roadblocks to clinical application of injectable protein delivery systems for sustained release. *J Pharm Sci*. 2012;101(3):946–954. doi:10.1002/jps.23018
24. Kumar M, Virmani T, Kumar G, et al. Nanocarriers in tuberculosis treatment: challenges and delivery strategies. *Pharmaceuticals*. 2023;16 (10):1360. doi:10.3390/PH16101360
25. Chaudhary KR, Puri V, Singh A, Singh C. A review on recent advances in nanomedicines for the treatment of pulmonary tuberculosis. *J Drug Deliv Sci Technol*. 2022;69:103069. doi:10.1016/J.JDDST.2021.103069
26. Nair A, Greeny A, Nandan A, et al. Advanced drug delivery and therapeutic strategies for tuberculosis treatment. *J Nanobiotechnol*. 2023;21 (1):1–31. doi:10.1186/S12951-023-02156-Y/FIGURES/7
27. Narum SM, Le T, Le DP, et al. Passive targeting in nanomedicine: fundamental concepts, body interactions, and clinical potential. *Nanopar Biomed Appl*. 2020:37–53. doi:10.1016/B978-0-12-816662-8.00004-7
28. Mazlan MKN, Tazizi MHDM, Ahmad R, et al. Antituberculosis targeted drug delivery as a potential future treatment approach. *Antibiotics*. 2021;10(8):908. doi:10.3390/ANTIBIOTICS10080908
29. Suresh AB, Rosani A, Patel P, Wadhwa R. Rifampin. *Encyclopedia Toxicol*. 2023;8:V8–305–V8–310. doi:10.1016/B978-0-12-824315-2.00695-3
30. Onzi G, Guterres SS, Pohlmann AR, Frank LA. Active targeting of nanocarriers. *ADME Encyclopedia*. 2021;1–13. doi:10.1007/978-3-030-51519-5_109-1
31. Gilbride B, Schmidt Garcia Moreira GM, Hust M, Cao C, Stewart L. Catalytic ferromagnetic gold nanoparticle immunoassay for the detection and differentiation of mycobacterium tuberculosis and mycobacterium bovis. *Anal Chim Acta*. 2021;1184:339037. doi:10.1016/J.ACA.2021.339037
32. Bai L, Chen Y, Bai Y, Chen Y, Zhou J, Huang A. Fullerene-doped polyaniline as new redox nanoprobe and catalyst in electrochemical aptasensor for ultrasensitive detection of mycobacterium tuberculosis MPT64 antigen in human serum. *Biomaterials*. 2017;133:11–19. doi:10.1016/J.BIOMATERIALS.2017.04.010
33. Huang H, Chen Y, Zuo J, et al. MXene-incorporated C60NPs and Au@Pt with dual-electric signal outputs for accurate detection of mycobacterium tuberculosis ESAT-6 antigen. *Biosens Bioelectron*. 2023;242:115734. doi:10.1016/J.BIOS.2023.115734
34. Chen Y, Guo S, Zhao M, et al. Amperometric DNA biosensor for mycobacterium tuberculosis detection using flower-like carbon nanotubes-polyaniline nanohybrid and enzyme-assisted signal amplification strategy. *Biosens Bioelectron*. 2018;119:215–220. doi:10.1016/J.BIOS.2018.08.023
35. Bakhori NM, Yusof NA, Abdullah J, Wasoh H, Rahman SKA, Rahman SFA. Surface enhanced CdSe/ZnS QD/SiNP electrochemical immunosensor for the detection of mycobacterium tuberculosis by combination of CFP10-ESAT6 for better diagnostic specificity. *Materials*. 2019;13(1):149. doi:10.3390/MA13010149
36. Maretti E, Costantino L, Rustichelli C, et al. Surface engineering of solid lipid nanoparticle assemblies by methyl α-d-mannopyranoside for the active targeting to macrophages in anti-tuberculosis inhalation therapy. *Int J Pharm*. 2017;528(1–2):440–451. doi:10.1016/J.IJPHARM.2017.06.045
37. Maretti E, Rustichelli C, Gualtieri ML, et al. The impact of lipid corona on rifampicin intramacrophagic transport using inhaled solid lipid nanoparticles surface-decorated with a mannosylated surfactant. *Pharmaceutics*. 2019;11(10):508. doi:10.3390/PHARMACEUTICS11100508
38. Mukhtar M, Csaba N, Robla S, et al. Dry powder comprised of isoniazid-loaded nanoparticles of hyaluronic acid in conjugation with mannose-anchored chitosan for macrophage-targeted pulmonary administration in tuberculosis. *Pharmaceutics*. 2022;14(8):1543. doi:10.3390/pharmaceutics14081543
39. Li B, Wang W, Zhao L, et al. Photothermal therapy of tuberculosis using targeting pre-activated macrophage membrane-coated nanoparticles. *Nature Nanotechnol*. 2024;19(6):834–845. doi:10.1038/s41565-024-01618-0
40. Fan S, Zhao D, Wang J, et al. Photothermal and host immune activated therapy of cutaneous tuberculosis using macrophage targeted mesoporous polydopamine nanoparticles. *Mater Today Bio*. 2024;28:101232. doi:10.1016/J.MTBIO.2024.101232
41. Mubin N, Umar MS, Zubair S, Owais M. Corrigendum: selective targeting of 4SO4-N-acetyl-galactosamine functionalized mycobacterium tuberculosis protein loaded chitosan nanoparticle to macrophages: correlation with activation of immune system (Front. Microbiol, (2018), 9, (2469). *Front Microbiol*. 2018;11:621067. doi:10.3389/FMICB.2020.621067/BIBTEX
42. Singh VK, Chau E, Mishra A, et al. CD44 receptor targeted nanoparticles augment immunity against tuberculosis in mice. *J Control Release*. 2022;349:796–811. doi:10.1016/J.JCONREL.2022.07.040
43. Gong Y, Jia H, Dang W, et al. Enhancing cell-mediated immunity through dendritic cell activation: the role of Tri-GalNAc-modified PLGA-PEG nanoparticles encapsulating SR717. *Front Immunol*. 2024;15:1490003. doi:10.3389/FIMMU.2024.1490003/BIBTEX
44. Shang S, Kats D, Cao L, et al. Induction of mycobacterium tuberculosislipid-specific t cell responses by pulmonary delivery of mycolic acid-loaded polymeric micellar nanocarriers. *Front Immunol*. 2018;9(NOV):393388. doi:10.3389/FIMMU.2018.02709/BIBTEX
45. Liang Q, Zhang P, Zhang L, et al. Development of tetracycline-modified nanoparticles for bone-targeted delivery of anti-tubercular drug. *Front Bioeng Biotechnol*. 2023;11:1207520. doi:10.3389/FBIOE.2023.1207520/BIBTEX
46. Garhyan J, Mohan S, Rajendran V, Bhatnagar R. Preclinical evidence of nanomedicine formulation to target mycobacterium tuberculosis at its bone marrow niche. *Pathogens*. 2020;9(5):372. doi:10.3390/PATHOGENS9050372
47. Prabhu P, Fernandes T, Chaubey P, et al. Mannose-conjugated chitosan nanoparticles for delivery of rifampicin to osteoarticular tuberculosis. *Drug Deliv Transl Res*. 2021;11(4):1509–1519. doi:10.1007/S13346-021-01003-7/METRICS
48. Li H, Ding Y, Huang J, et al. Angiopep-2 modified exosomes load rifampicin with potential for treating central nervous system tuberculosis. *Int J Nanomed*. 2023;18:489–503. doi:10.2147/IJN.S395246
49. de Castro RR, Do Carmo FA, Martins C, et al. Clofazimine functionalized polymeric nanoparticles for brain delivery in the tuberculosis treatment. *Int J Pharm*. 2021;602:120655. doi:10.1016/J.IJPHARM.2021.120655
50. Domagk G. Investigations on the antituberculous activity of the thiosemicarbazones in vitro and in vivo. *Am Rev Tuberc*. 1950;61(1):8–19. doi:10.1164/ART.1950.61.1.8
51. Horváti K, Bacsa B, Szabó N, et al. Antimycobacterial activity of peptide conjugate of pyridopyrimidine derivative against mycobacterium tuberculosis in a series of in vitro and in vivo models. *Tuberculosis*. 2015;95(S1):S207–S211. doi:10.1016/J.TUBE.2015.02.026
52. Pawde DM, Viswanadh MK, Mehata AK, et al. Mannose receptor targeted bioadhesive chitosan nanoparticles of clofazimine for effective therapy of tuberculosis. *Saudi Pharm J*. 2020;28(12):1616–1625. doi:10.1016/J.JSPS.2020.10.008

53. Maurya P, Saklani R, Singh S, et al. Appraisal of fluoroquinolone-loaded carubinose-linked hybrid nanoparticles for glycotargeting to alveolar macrophages. *Drug Deliv Transl Res*. 2022;12(7):1640–1658. doi:10.1007/S13346-021-01055-9/METRICS
54. Liao K, Chen R, Zhang J, et al. cGAS-mediated antibacterial immunotherapy against tuberculosis by macrophage-targeted manganese dioxide nanoagonist. *Acta Biomater*. 2025;196:471–486. doi:10.1016/J.ACTBIO.2025.03.002
55. Vieira ACC, Magalhães J, Rocha S, et al. Targeted macrophages delivery of rifampicin-loaded lipid nanoparticles to improve tuberculosis treatment. *Nanomedicine*. 2017;12(24):2721–2736. doi:10.2217/NNM-2017-0248;SUBPAGE:STRING:ACCESS
56. Choi SR, Britigan BE, Moran DM, Narayanasamy P. Gallium nanoparticles facilitate phagosome maturation and inhibit growth of virulent mycobacterium tuberculosis in macrophages. *PLoS One*. 2017;12(5):e0177987. doi:10.1371/JOURNAL.PONE.0177987
57. Pinheiro M, Ribeiro R, Vieira A, Andrade F, Reis S. Design of a nanostructured lipid carrier intended to improve the treatment of tuberculosis. *Drug Des Devel Ther*. 2016;10:2467–2475. doi:10.2147/DDDT.S104395
58. Ravindran R, Mitra K, Arumugam SK, Doble M. Preparation of curdlan sulphate - chitosan nanoparticles as a drug carrier to target mycobacterium smegmatis infected macrophages. *Carbohydr Polym*. 2021;258:117686. doi:10.1016/J.CARBPOL.2021.117686
59. Horváti K, Gyulai G, Csámpai A, Rohonczy J, Kiss É, Bösze S. Surface layer modification of poly(d, l -lactic- co-glycolic acid) nanoparticles with targeting peptide: a convenient synthetic route for pluronic F127-tuftsin conjugate. *Bioconjug Chem*. 2018;29(5):1495–1499. doi:10.1021/ACS.BIOCONJCHEM.8B00156/SUPPL_FILE/BC8B00156_SI_001.PDF
60. Gao Y, Sarfraz MK, Clas SD, Roa W, Löbenberg R. Hyaluronic acid-tocopherol succinate-based self-assembling micelles for targeted delivery of rifampicin to alveolar macrophages. *J Biomed Nanotechnol*. 2014;11(8):1312–1329. doi:10.1166/JBN.2015.2091
61. Tukulula M, Gouveia L, Paixao P, Hayeshi R, Naicker B, Dube A. Functionalization of PLGA nanoparticles with 1,3-β-glucan enhances the intracellular pharmacokinetics of rifampicin in macrophages. *Pharm Res*. 2018;35(6):1–11. doi:10.1007/S11095-018-2391-8/FIGURES/8
62. Lemmer Y, Kalombo L, Pietersen RD, et al. Mycolic acids, a promising mycobacterial ligand for targeting of nanoencapsulated drugs in tuberculosis. *J Control Release*. 2015;211:94–104. doi:10.1016/J.JCONREL.2015.06.005
63. Pati R, Sahu R, Panda J, Sonawane A. Encapsulation of zinc-rifampicin complex into transferrin-conjugated silver quantum-dots improves its antimycobacterial activity and stability and facilitates drug delivery into macrophages. *Sci Rep*. 2016;6(1):6. doi:10.1038/SREP24184
64. O'Connor C, Patel P, Brady FM. Isoniazid. *Encyclopedia Toxicol*. 2024;5:V5–701–V5–706. doi:10.1016/B978-0-12-824315-2.00121-4
65. Arca HÇ, Mosquera-Giraldo LI, Pereira JM, Sriranganathan N, Taylor LS, Edgar KJ. Rifampin stability and solution concentration enhancement through amorphous solid dispersion in cellulose ω-carboxyalkanoate matrices. *J Pharm Sci*. 2018;107(1):127–138. doi:10.1016/J.XPHS.2017.05.036
66. Chakraborty S, Rhee KY. Tuberculosis drug development: history and evolution of the mechanism-based paradigm. *Cold Spring Harb Perspect Med*. 2015;5(8):1–11. doi:10.1101/CSHPERSPECT.A021147
67. Mwila C, Walker RB. Improved stability of rifampicin in the presence of gastric-resistant isoniazid microspheres in acidic media. *Pharmaceutics*. 2020;12(3):234. doi:10.3390/PHARMACEUTICS12030234
68. Zumla A, Chakaya J, Centis R, et al. Tuberculosis treatment and management-an update on treatment regimens, trials, new drugs, and adjunct therapies. *Lancet Respir Med*. 2015;3(3):220–234. doi:10.1016/S2213-2600(15)00063-6
69. Ostrovskii KP, Osipova NS, Vanchugova LV, et al. Use of proteins to increase the aqueous solubility of rifapentine. *Pharm Chem J*. 2016;50(6):407–412. doi:10.1007/s11094-016-1460-8
70. Kalra JM, Kalra K, Pokhriyal V, Husaain K. Solubility enhancement of rifabutin by co-solvency approach. *J Pharm Negat Results*. 2022;1748–1754. doi:10.47750/PNR.2022.13.S09.210
71. British Columbia Centre. Therapeutic guidelines for opportunistic infections mycobacterium avium complex (MAC); 2023. Available from: https://bccfe.ca/wp-content/uploads/2024/04/bc-cfe_therapeutic_guidelines_for_opportunistic_infections-mac-mar-2023.pdf. Accessed June 13, 2025.
72. Crabol Y, Catherinot E, Veziris N, Jullien V, Lortholary OR. Where do we stand in 2016? *J Antimicrob Chemother*. 2016;71(7):1759–1771. doi:10.1093/JAC/DKW024
73. Podder V, Patel P, Sadiq NM. *Levofloxacin Kucers the Use of Antibiotics: a Clinical Review of Antibacterial, Antifungal, Antiparasitic, and Antiviral Drugs*. 7th ed. 2024:2055–2084. doi:10.1201/9781315152110
74. Christof C, Nußbaumer-Streit B, Gartlehner G. WHO guidelines on tuberculosis infection prevention and control. *Gesundheitswesen*. 2020;82(11):885–889. doi:10.1055/A-1241-4321/ID/R2020-05-1160-0007/BIB
75. Salem II, Steffan G, Düzgünes N. Efficacy of clofazimine-modified cyclodextrin against mycobacterium avium complex in human macrophages. *Int J Pharm*. 2003;260(1):105–114. doi:10.1016/S0378-5173(03)00236-9
76. Sousa ML, Sarraguça MC, Oliveira Dos Santos A, et al. A new salt of clofazimine to improve leprosy treatment. *J Mol Struct*. 2020;1214:128226. doi:10.1016/J.MOLSTRUC.2020.128226
77. Churilov L, Korzhikov-Vlakh V, Sinitsyna E, et al. Enhanced delivery of 4-thioureidoiminomethylpyridinium perchlorate in tuberculosis models with IgG functionalized poly(lactic acid)-based particles. *Pharmaceutics*. 2018;11(1):2. doi:10.3390/PHARMACEUTICS11010002
78. Li F, Liu F, Huang K, Yang S. Advancement of gallium and gallium-based compounds as antimicrobial agents. *Front Bioeng Biotechnol*. 2022;10:827960. doi:10.3389/FBIOE.2022.827960/BIBTEX
79. Leyland-Jones B. Treatment of cancer-related hypercalcemia: the role of gallium nitrate. *Semin Oncol*. 2003;30(2 SUPPL. 5):13–19. doi:10.1016/S0093-7754(03)00171-4
80. Najahi-Missaoui W, Arnold RD, Cummings BS. Safe nanoparticles: are we there yet? *Int J Mol Sci*. 2021;22(1):1–22. doi:10.3390/IJMS22010385
81. Siddique S, Chow JCL. Application of nanomaterials in biomedical imaging and cancer therapy. *Nanomaterials*. 2020;10(9):1–41. doi:10.3390/NANO10091700
82. Vollath D. *Nanomaterials: An Introduction to Synthesis, Properties, and Applications*. Second. Wiley-VCH Verlag GmbH & Co. KGaA; 2013. Accessed June 15, 2025. https://www.phy.pmf.unizg.hr/~dpajic/buksa/nanomaterijali/Nanomaterials-An-Introduction-to-Synthesis-Properties-and-Applications.pdf.
83. Pang J, Mendes RG, Bachmatiuk A, et al. Applications of 2D MXenes in energy conversion and storage systems. *Chem Soc Rev*. 2019;48(1):72–133. doi:10.1039/C8CS00324F
84. Zainon NKR, Abdullah CAC, Jamaludin NS. Toxicity of nanomaterials. *Handbook Green Sustain Nanotechnol*. 2022;1–21. doi:10.1007/978-3-030-69023-6_37-1

85. Naguib M, Kurtoglu M, Presser V, et al. Two-dimensional nanocrystals produced by exfoliation of Ti3AlC2. *Adv Mater*. 2011;23(37):4248–4253. doi:10.1002/ADMA.201102306
86. Molaei MJ. Carbon quantum dots and their biomedical and therapeutic applications: a review. *RSC Adv*. 2019;9(12):6460–6481. doi:10.1039/C8RA08088G
87. Mekuye B, Abera B. Nanomaterials: an overview of synthesis, classification, characterization, and applications. *Nano Select*. 2023;4(8):486–501. doi:10.1002/NANO.202300038
88. Naief MF, Mohammed SN, Mayouf HJ, Mohammed AM. A review of the role of carbon nanotubes for cancer treatment based on photothermal and photodynamic therapy techniques. *J Organomet Chem*. 2023;999:122819. doi:10.1016/J.JORGANCHEM.2023.122819
89. Kelíšková P, Matvieiev O, Janíková L, Šelešovská R. Recent advances in the use of screen-printed electrodes in drug analysis: a review. *Curr Opin Electrochem*. 2023;42:101408. doi:10.1016/J.COELEC.2023.101408
90. Ivanov R, Czibula C, Teichert C, Bojinov M, Tsakova V. Carbon screen-printed electrodes for substrate-assisted electroless deposition of palladium. *J Electroanal Chem*. 2021;897:115617. doi:10.1016/J.JELECHEM.2021.115617
91. Saleh M, Gul A, Nasir A, Moses TO, Nural Y, Yabalak E. Comprehensive review of carbon-based nanostructures: properties, synthesis, characterization, and cross-disciplinary applications. *J Ind Eng Chem*. 2025;146:176–212. doi:10.1016/J.JIEC.2024.11.052
92. Alshawwa SZ, Kassem AA, Farid RM, Mostafa SK, Labib GS. Nanocarrier drug delivery systems: characterization, limitations, future perspectives and implementation of artificial intelligence. *Pharmaceutics*. 2022;14(4):883. doi:10.3390/PHARMACEUTICS14040883
93. Sinani G, Sessevmez M, Şenel S. Applications of chitosan in prevention and treatment strategies of infectious diseases. *Pharmaceutics*. 2024;16(9):1201. doi:10.3390/PHARMACEUTICS16091201
94. Merisko-Liversidge EM, Liversidge GG. Drug nanoparticles: formulating poorly water-soluble compounds. *Toxicol Pathol*. 2008;36(1):43–48. doi:10.1177/0192623307310946
95. Li B, Wang W, Song W, et al. Antiviral and anti-inflammatory treatment with multifunctional alveolar macrophage-like nanoparticles in a surrogate mouse model of COVID-19. *Adv Sci*. 2021;8(13). doi:10.1002/ADVS.202003556
96. Wang W, Li B, Wu Y, et al. Macrophage-derived biomimetic nanoparticles for light-driven theranostics toward Mpox. *Matter*. 2024;7(3):1187–1206. doi:10.1016/j.matt.2024.01.004
97. WHO. 2024 Global tuberculosis report; 2024.
98. Kiss É, Gyulai G, Pénzes CB, et al. Tuneable surface modification of PLGA nanoparticles carrying new antitubercular drug candidate. *Colloids Surf a Physicochem Eng Asp*. 2014;458(1):178–186. doi:10.1016/J.COLSURFA.2014.05.048
99. Varga B, Barabás O, Takács E, Nagy N, Nagy P, Vértessy BG. Active site of mycobacterial dUTPase: structural characteristics and a built-in sensor. *Biochem Biophys Res Commun*. 2008;373(1):8–13. doi:10.1016/j.bbrc.2008.05.130
100. Day NJ, Abt MC. Trends in microbiology | 32, 3, e1-e2, 219-316 (March 2024) | scienceDirect.com by Elsevier. *Trends Microbiol*. 2024;32(3):219–316. doi:10.1016/j.tim.2024.01.006
101. Horváti K, Bacsa B, Szabó N, et al. Enhanced cellular uptake of a new, in silico identified antitubercular candidate by peptide conjugation. *Bioconjug Chem*. 2012;23(5):900–907. doi:10.1021/BC200221T
102. Hammouda MM, Rashed MM, Elattar KM, Osman AMA. Synthetic strategies of heterocycle-integrated pyridopyrimidine scaffolds supported by nano-catalysts. *RSC Adv*. 2023;13(17):11600. doi:10.1039/D3RA00922J
103. Tadele S, Girmay S. Quantification of bioactive constituent D-pinitol in ethiopian soybean. *Nat Prod Chem Res*. 2018;6(2):1–4. doi:10.4172/2329-6836.1000313
104. Aziz Ibrahim IA, Alzahrani AR, Alanazi IM, et al. Bioactive compound D-Pinitol-loaded graphene oxide-chitosan-folic acid nanocomposite induced apoptosis in human hepatoma HepG-2 cells. *J Drug Deliv Sci Technol*. 2024;92:105282. doi:10.1016/J.JDDST.2023.105282
105. Taki A, Smooker P. Small wonders—the use of nanoparticles for delivering antigen. *Vaccines*. 2015;3(3):638–661. doi:10.3390/VACCINES3030638
106. Belay M, Legesse M, Mihret A, et al. Pro- and anti-inflammatory cytokines against Rv2031 are elevated during latent tuberculosis: a study in cohorts of tuberculosis patients, household contacts and community controls in an endemic setting. *PLoS One*. 2015;10(4):e0124134. doi:10.1371/JOURNAL.PONE.0124134
107. Zhang Z, Xu L, Wang X, et al. Construction and expression of mycobacterium tuberculosis fusion protein SHR3 and its immunogenicity analysis in combination with various adjuvants. *Tuberculosis*. 2024;145:102480. doi:10.1016/J.TUBE.2024.102480
108. Cai J, Wang H, Wang D, Li Y. Improving cancer vaccine efficiency by nanomedicine. *Adv Biosyst*. 2019;3(3). doi:10.1002/ADBI.201800287
109. Zhao J, Siddiqui S, Shang S, et al. Mycolic acid-specific T cells protect against mycobacterium tuberculosis infection in a humanized transgenic mouse model. *Elife*. 2015;4(DECEMBER2015). doi:10.7554/ELIFE.08525
110. De Libero G, Mori L. The T-cell response to lipid antigens of mycobacterium tuberculosis. *Front Immunol*. 2014;5(MAY):1. doi:10.3389/FIMMU.2014.00219/XML/NLM
111. Est-Witte SE, Livingston NK, Omotoso MO, Green JJ, Schneck JP. Nanoparticles for generating antigen-specific T cells for immunotherapy. *Semin Immunol*. 2021;56:101541. doi:10.1016/J.SMIM.2021.101541
112. Costa-Gouveia J, Aínsa JA, Brodin P, Lucía A. How can nanoparticles contribute to antituberculosis therapy? *Drug Discov Today*. 2017;22(3):600–607. doi:10.1016/j.drudis.2017.01.011
113. Virmani T, Kumar G, Virmani R, Sharma A, Pathak K. Nanocarrier-based approaches to combat chronic obstructive pulmonary disease. *Nanomedicine*. 2022;17(24):1833–1854. doi:10.2217/NNM-2021-0403
114. Luo Y. Perspectives on important considerations in designing nanoparticles for oral delivery applications in food. *J Agric Food Res*. 2020;2:100031. doi:10.1016/J.JAFR.2020.100031
115. Wakekar S, Tiwari A, Chaskar J, Chaskar A. Protein nanotubes as drug delivery systems: an overview. *J Nanopart Res*. 2023;25(7). doi:10.1007/S11051-023-05786-3
116. Virmani T, Kumar G, Sharma A, et al. Amelioration of cancer employing chitosan, its derivatives, and chitosan-based nanoparticles: recent updates. *Polymers*. 2023;15(13):2928. doi:10.3390/POLYM15132928
117. Pandey R, Sharma A, Zahoor A, Sharma S, Khuller GK, Prasad B. Poly (DL-lactide-co-glycolide) nanoparticle-based inhalable sustained drug delivery system for experimental tuberculosis. *J Antimicrob Chemother*. 2003;52(6):981–986. doi:10.1093/JAC/DKG477

118. Colone M, Calcabrini A, Stringaro A. Drug delivery systems of natural products in oncology. *Molecules*. 2020;25(19):4560. doi:10.3390/MOLECULES25194560
119. Araujo VHS, Delello Di Filippo L, Duarte JL, et al. Exploiting solid lipid nanoparticles and nanostructured lipid carriers for drug delivery against cutaneous fungal infections. *Crit Rev Microbiol*. 2021;47(1):79–90. doi:10.1080/1040841X.2020.1843399
120. Sumera AA, Ovais M, Raza A, Raza A, Raza A. Docetaxel-loaded solid lipid nanoparticles: a novel drug delivery system. *IET Nanobiotechnol*. 2017;11(6):621–629. doi:10.1049/IET-NBT.2017.0001
121. Hosseini SM, Taheri M, Nouri F, Farmani A, Moez NM, Arabestani MR. Nano drug delivery in intracellular bacterial infection treatments. *Biomed Pharmacother*. 2022;146. doi:10.1016/j.biopha.2021.112609
122. Gothwal A, Khan I, Gupta U. Polymeric micelles: recent advancements in the delivery of anticancer drugs. *Pharm Res*. 2016;33(1):18–39. doi:10.1007/S11095-015-1784-1
123. Mishra V, Bansal KK, Verma A, et al. Solid lipid nanoparticles: emerging colloidal nano drug delivery systems. *Pharmaceutics*. 2018;10(4):191. doi:10.3390/PHARMACEUTICS10040191
124. Baek JS, Na YG, Cho CW. Sustained cytotoxicity of wogonin on breast cancer cells by encapsulation in solid lipid nanoparticles. *Nanomaterials*. 2018;8(3):159. doi:10.3390/NANO8030159
125. Sharma A, Goyal AK, Rath G. Recent advances in metal nanoparticles in cancer therapy. *J Drug Target*. 2018;26(8):617–632. doi:10.1080/1061186X.2017.1400553
126. Carnero Canales CS, Marquez Cazorla JI, Marquez Cazorla RM, et al. Breaking barriers: the potential of nanosystems in antituberculosis therapy. *Bioact Mater*. 2024;39:106–134. doi:10.1016/J.BIOACTMAT.2024.05.013
127. Moku G, Gopalsamuthiram VR, Hoye TR, Panyam J. Surface modification of nanoparticles: methods and applications. In: *Surface modification of polymers: methods and applications*. 2019:317–346. doi:10.1002/9783527819249.CH11
128. Sung Y, Choi Y, Kim ES, Ryu JH, Kwon IC. Receptor-ligand interactions for optimized endocytosis in targeted therapies. *J Control Release*. 2025;380:524–538. doi:10.1016/J.JCONREL.2025.01.060
129. Patel P, Hanini A, Shah A, et al. Surface modification of nanoparticles for targeted drug delivery. Surface modification of nanoparticles for targeted drug delivery. *BMC Complement Alternat Med*. 2019;19(1):19–31. doi:10.1007/978-3-030-06115-9_2
130. Suk JS, Xu Q, Kim N, Hanes J, Ensign LM. PEGylation as a strategy for improving nanoparticle-based drug and gene delivery. *Adv Drug Deliv Rev*. 2016;99(Pt A):28–51. doi:10.1016/J.ADDR.2015.09.012
131. Ahmad J, Garg A, Mustafa G, Ahmad MZ, Aslam M, Mishra A. Hybrid quantum dot as promising tools for theranostic application in cancer. *Electronics*. 2023;12(4):972. doi:10.3390/ELECTRONICS12040972
132. Sun M, Qu S, Hao Z, et al. Towards efficient solid-state photoluminescence based on carbon-nanodots and starch composites. *Nanoscale*. 2014;6(21):13076–13081. doi:10.1039/C4NR04034A
133. PD L, KN L, Phan HL, Nguyen HHT, Duong VA, Nguyen HV. Recent advances in surface decoration of nanoparticles in drug delivery. *Front Nanotechnol*. 2024;6:1456939. doi:10.3389/FNANO.2024.1456939/XML/NLM
134. Tian N, Duan H, Cao T, et al. Macrophage-targeted nanoparticles mediate synergistic photodynamic therapy and immunotherapy of tuberculosis. *RSC Adv*. 2023;13(3):1727–1737. doi:10.1039/D2RA06334D
135. Qie Y, Yuan H, Von Roemeling CA, et al. Surface modification of nanoparticles enables selective evasion of phagocytic clearance by distinct macrophage phenotypes. *Sci Rep*. 2016;6(1):6. doi:10.1038/SREP26269
136. Zhang H, Liu J, Chen Q, Mi P. Ligand-installed anti-VEGF genomic nanocarriers for effective gene therapy of primary and metastatic tumors. *J Control Release*. 2020;320:314–327. doi:10.1016/j.jconrel.2020.01.026
137. Mehta M, Bui TA, Yang X, Aksoy Y, Goldys EM, Deng W. Lipid-based nanoparticles for drug/gene delivery: an overview of the production techniques and difficulties encountered in their industrial development. *ACS Materials Au*. 2023;3(6):600–619. doi:10.1021/ACSMATERIALSAU.3C00032/ASSET/IMAGES/LARGE/MG3C00032_0004.JPEG
138. Yi YS. Folate receptor-targeted diagnostics and therapeutics for inflammatory diseases. *Immune Netw*. 2016;16(6):337–343. doi:10.4110/IN.2016.16.6.337
139. Abdellatif Ah AH, Tawfeek HM, Younis MA, Alsharidah M, Al Rugaie O. Biomedical applications of quantum dots: overview, challenges, and clinical potential. *Int J Nanomed*. 2022;17:1951–1970. doi:10.2147/IJN.S357980
140. Latha BD, Soumya K, More N, et al. Fluorescent carbon quantum dots for effective tumor diagnosis: a comprehensive review. *Biomed Engine Adv*. 2023;5:100072. doi:10.1016/J.BEA.2023.100072
141. Hanmante PS, Lohiya RT, Wankhede AG, et al. Quantum dot nanotechnology: advancing target drug delivery in oncology. *Next Nanotechnol*. 2025;7:100172. doi:10.1016/J.NXNANO.2025.100172
142. Bi J, Mo C, Li S, et al. Immunotoxicity of metal and metal oxide nanoparticles: from toxic mechanisms to metabolism and outcomes. *Biomater Sci*. 2023;11(12):4151–4183. doi:10.1039/D3BM00271C
143. Zhu C, Chen Z, Gao S, et al. Recent advances in non-toxic quantum dots and their biomedical applications. *Prog Nat Sci Mater Int*. 2019;29(6):628–640. doi:10.1016/J.PNSC.2019.11.007
144. Zhong H, Liu C, Ge W, Sun R, Huang F, Wang X. Self-assembled conjugated polymer/chitosan- graft -oleic acid micelles for fast visible detection of aliphatic biogenic amines by "turn-on" FRET. *ACS Appl Mater Interfaces*. 2017;9(27):22875–22884. doi:10.1021/ACSAMI.7B06168
145. Zlotnikov ID, Ezhov AA, Kudryashova EV. pH-sensitive fluorescent marker based on rhodamine 6g conjugate with its FRET/PeT pair in "smart" polymeric micelles for selective imaging of cancer cells. *Pharmaceutics*. 2024;16(8):1007. doi:10.3390/pharmaceutics16081007
146. Ju S, Cho H-Y. Biohybrid nanoparticle-based in situ monitoring of in vivo drug delivery. *Biosensors*. 2023;13(12):1017. doi:10.3390/BIOS13121017
147. Wang W, Mo W, Xiao X, et al. Antibiotic-loaded lactoferrin nanoparticles as a platform for enhanced infection therapy through targeted elimination of intracellular bacteria. *Asian J Pharm Sci*. 2024;19(4):100926. doi:10.1016/J.AJPS.2024.100926
148. Mobed A, Darvishi M, Kohansal F, et al. Biosensors; nanomaterial-based methods in diagnosing of mycobacterium tuberculosis. *J Clin Tuberc Other Mycobact Dis*. 2024;34:100412. doi:10.1016/J.JCTUBE.2023.100412
149. Fu Z, Hou Y, Haugen HJ, et al. TiO2 nanostructured implant surface-mediated M2c polarization of inflammatory monocyte requiring intact cytoskeleton rearrangement. *J Nanobiotechnol*. 2023;21(1):1–31. doi:10.1186/s12951-022-01751-9

150. Hassett KJ, Benenato KE, Jacquinet E, et al. Optimization of lipid nanoparticles for intramuscular administration of mRNA vaccines. *Mol Ther Nucleic Acids*. 2019;15:1–11. doi:10.1016/j.omtn.2019.01.013
151. Kole S, Qadiri SSN, Shin S-M, Kim W-S, Lee J, Jung S-J. PLGA encapsulated inactivated-viral vaccine: formulation and evaluation of its protective efficacy against viral haemorrhagic septicaemia virus (VHSV) infection in olive flounder (Paralichthys olivaceus) vaccinated by mucosal delivery routes. *Vaccine*. 2019;37(7):973–983. doi:10.1016/j.vaccine.2018.12.063
152. Baranyai Z, Soria-Carrera H, Alleva M, et al. Nanotechnology-based Targeted drug delivery: an emerging tool to overcome tuberculosis. *Adv Therapeutics*. 2021;4(1):2000113. doi:10.1002/adtp.202000113